EXPERIMENTAL INVESTIGATION OF HEAT TRANSFER ENHANCEMENT OF NANOFLUIDS IN COMPUTER COOLING SYSTEMS

by

Özgür Atik

B.S., Mechanical Engineering, İzmir Institute of Technology, 2013

Submitted to the Institute for Graduate Studies in
Science and Engineering in partial fulfillment of
the requirements for the degree of
Master of Science

Graduate Program in Mechanical Engineering
Boğaziçi University

2017

ACKNOWLEDGEMENTS

First and foremost, I would like to express my sincerest gratitude to my supervisor, Assoc. Prof. Hakan Ertürk for his endless support, encouragement, and immense knowledge. I am grateful for all his contributions of time, ideas, and guidance to make my master study experience productive and stimulating.

Besides my advisor, I am grateful to my committee members Assoc. Prof. Hasan Bedir and Assist. Prof. Altuğ Melik Başol for their time, insightful comments and constructive criticism for my study.

I would like to thank Boğaziçi University for support under B.U. Research Fund AP-10061.

I would also like to thank my lab mate, Beybin İlhan for her endless support, encouragement and friendship through the my process of researching and experimenting. I am also thankful to my dearest friends; Çağlayan Adıgüzel, Hasan Alparslan and Nazlı Turan for their valuable friendship and all the greatest times we have spent together.

Finally, I would like to thank my family; Ayşe Atik, Ahmet Atik and Elif Öznur Atik for their continuous and unparalleled love. They have always believed in me and supported me at my each step.

ABSTRACT

EXPERIMENTAL INVESTIGATION OF HEAT TRANSFER ENHANCEMENT OF NANOFLUIDS IN COMPUTER COOLING SYSTEMS

In this study, cooling performance enhancement of computer liquid cooling systems using hBN-water nanofluids are investigated experimentally. Water based nanofluids are prepared with two step method by using ultrasonication and surface active materials. The particle volume fractions of 0.1-2% are considered at constant flow rates varying from 0.3-2 L/min for experimental systems with two different cold plates. A commercial closed loop liquid cooling system is also tested to examine performance of hBN-water nanofluids at constant pumping power. It is observed that the maximum cooling enhancement is obtained with 2% volume concentration of hBN-water nanofluid in all experimental systems and reduction in the thermal resistance of liquid cooling systems and Stanton number are correlated at constant flow rate experiments. Moreover, enhancement rate of cooling performance depends on the flow rate and the cold plate design. The cooling performance increase for the commercial system is observed to be limited with the reduced flow rate at increasing particle volume fractions. Therefore, cold plates must be optimized to maximize the cooling capacity, considering the increasing viscosity and thermal conductivity of nanofluids.

ÖZET

NANOAKIŞKANLARIN BİLGİSAYAR SOĞUTMA SİSTEMLERİNDEKİ ISI TRANSFERİ ARTTIRIMININ DENEYSEL OLARAK İNCELENMESİ

Bu çalışmada hBN-su nanoakışkanları kullanılan bilgisayar sıvı soğutma sistemlerinin soğutma performans artışı deneysel olarak incelenmiştir. Su bazlı nanoakışkanlar ultrasonik karıştırma yöntemi ve yüzey aktif madde kullanımı baz alınarak 2 adımlı üretim yöntemiyle üretilmiştir. İki farklı soğutma plakasının kullanıdığı deneysel sistemlerde 0.1-2% parçacık hacim fraksiyonları için değelendirmeler 0.3-2 L/dk arası değişen sabit akış debilerinde yapılmıştır. Ayrıca ticari amaçlı üretilmiş kapalı devre sıvı soğutma sistemi hBN-su nanoakışkanlarının performansını incelemek için sabit pompa gücünde test edilmiştir. Yapılan tüm deneylerin sonucunda maksimum soğutma artış oranı 2% hacim konsantrasyonuna sahip hBN-su nanoakışkanı ile elde edilmiş olup, sabit debide geçerkleştirilen deneylerde Stanton sayısı ve sıvı soğutma sistemlerinin ısıl direncindeki azalmanın ilişkili olduğunu gözlemlenmiştir. Buna ek olarak, soğutma performansındaki artış oranı akış debisi ve soğutma plakası tasarımına bağlıdır. Artan parçacık fraksyonları ile yapılan deneylerde, ticari sistemdeki soğutma performansı artışının azalan akış debisi ile kısıtlı olduğu gözlemlenmiştir. Bu sebeple, nanoakışkanların viskozite ve ısı iletkenliğindeki artış dikkate alındığında, soğutma kapasitesini maksimuma çıkarmak için en uygun soğutma plakası kullanılmalıdır.

TABLE OF CONTENTS

ACKNOWLEDGEMENTS iii
ABSTRACT iv
ÖZET v
LIST OF FIGURES viii
LIST OF TABLES xi
LIST OF SYMBOLS xii
LIST OF ACRONYMS/ABBREVIATIONS xiv
1. INTRODUCTION 1
 1.1. Problem Overview 1
 1.2. Cooling Techniques 3
  1.2.1. Radiation and Natural Convection Cooling 3
  1.2.2. Forced Air Cooling 5
  1.2.3. Forced Liquid Cooling 6
   1.2.3.1. Liquid Coolants 6
 1.3. Nanofluids 7
 1.4. Literature Survey 8
 1.5. Objective 12
2. METHODOLOGY 14
 2.1. Experimental Procedure 14
  2.1.1. Nanofluid Preparation 14
  2.1.2. Thermal Conductivity Measurement 15
  2.1.3. Viscosity Measurements 16
  2.1.4. Experimental Systems 16
   2.1.4.1. First Experimental System 17
   2.1.4.2. Second Experimental System 22
  2.1.5. Data Analysis 24
   2.1.5.1. Experimental Uncertainties 26
3. EXPERIMENTS AND RESULTS 27
 3.1. Thermal Conductivity and Viscosity of Nanofluids 27

3.2. Experimental Results 28
3.2.1. Results of First Experimental System 28
3.3. Results of Second Experimental System 33
4. CONCLUSION AND FUTURE WORK 39
4.1. Conclusion 39
4.2. Recommendations for Future Work 40
REFERENCES 41
APPENDIX A: TECHNICAL DRAWINGS 49

LIST OF FIGURES

Figure 1.1. Change of the transistor count in a microprocessor over the past years . . . 2

Figure 1.2. A CPU of a computer before and after overheating failure . . . 3

Figure 1.3. Heat transfer performance of cooling techniques . . . 4

Figure 1.4. Different heat sinks used in natural convection cooling technique . 4

Figure 1.5. Different heat sink and fan cofigurations used in forced air cooling technique . . . 5

Figure 1.6. Schematic diagram of simple forced liquid cooling system . . . 6

Figure 1.7. Commercial liquid cooling systems . . . 7

Figure 2.1. First experimental system . . . 17

Figure 2.2. Schematic diagram of first experimental system . . . 18

Figure 2.3. Copper heater block . . . 18

Figure 2.4. Temperature distribution in heater block . . . 19

Figure 2.5. Sections of heater block and locations of thermocouples . . . 20

Figure 2.6. Finned cold plate . . . 20

Figure 2.7. Flat cold plate 21

Figure 2.8. Heat exchanger mounted in the middle of wind tunnel 21

Figure 2.9. Commercial cold plate 22

Figure 2.10. Second experimental system 23

Figure 2.11. Schematic diagram of second experimental system 23

Figure 3.1. The change in nanofluid to base fluid viscosity and thermal conductivity ratios of Al_2O_3 and hBN nanofluids 27

Figure 3.2. The change in case-to-ambient thermal resistance of first experimental system with flat cold plate 29

Figure 3.3. The change in thermal resistance of flat cold plate 30

Figure 3.4. The change in heat exchanger thermal resistance of first experimental system with flat cold plate 30

Figure 3.5. The change in case-to-ambient thermal resistance of first experimental system with finned cold plate 31

Figure 3.6. The change in thermal resistance of finned cold plate 32

Figure 3.7. The change in heat exchanger thermal resistance of first experimental system with finned cold plate 32

Figure 3.8. The change in case-to-ambient thermal resistance of second experimental system 34

Figure 3.9. The change in cold plate thermal resistance of second experimental system 34

Figure 3.10. The change in heat exchanger thermal resistance of second experimental system 35

Figure 3.11. Effect of particle volume fraction of nanofluids on volume flow rate, case-to-ambient thermal resistance and cold plate thermal resistance 36

Figure 3.12. The change in normalized Stanton number for cold plate type, flow rate and hBN volume concentration 37

Figure 3.13. Enhancement rates of Stanton number and case-to-ambient thermal resistance for different volume concentrations of hBN-water nanofluids and volume flow rates 38

Figure A.1. Technical drawing of copper heater block 49

LIST OF TABLES

Table 2.1. Details of nanofluid preparation 15

Table 2.2. Details of experimental conditions 16

LIST OF SYMBOLS

A_{neck}	Cross section area of the neck section of heater
$c_{p,bf}$	Heat capacity of the base fluid
$c_{p,p}$	Heat capacity of the particle
$c_{p,nf}$	Heat capacity of the nanofluid
E	Enhancement rate
k	Thermal conductivity of copper
k_{bf}	Thermal conductivity of base fluid
k_{nf}	Thermal conductivity of nanofluid
q	Heat load
Re	Reynolds number
St	Stanton number
T_a	Ambient temperature
T_c	Case temperature
T_{h1}	Temperature of the first hole of copper heater
T_{h2}	Temperature of the second hole of copper heater
T_i	Inlet temperature
T_o	Outlet temperature
UA	Overall heat transfer coefficient times heat transfer area
$\dot{V}$	Volume flow rate

ΔT_{lm}	Log-mean temperature
Δx	Distance between T_{h1} and T_{h2}
φ	Particle volume fraction of the nanofluid
μ_{bf}	Viscosity of base fluid
μ_{nf}	Viscosity of nanofluid
σ_q	Uncertainty of heat load
σ_T	Uncertainty of thermocouple
$\sigma_{\theta_{c-a}}$	Uncertainty of case-to-ambient thermal resistance

$\sigma_{\dot{V}}$	Uncertainty of volume flow rate
σ_x	Uncertainty of caliper
θ_{bf}	Thermal resistance of base fluid
θ_{c-a}	Case-to-ambient thermal resistance
θ_{c-i}	Thermal resistance of cold plate
θ_{i-o}	Thermal resistance of flow
θ_{nf}	Thermal resistance of nanofluid
θ_{o-a}	Thermal resistance of heat exchanger
$\rho_{p,bf}$	Density of the base fluid
$\rho_{p,p}$	Density of the particle
$\rho_{p,nf}$	Density of the nanofluid

LIST OF ACRONYMS/ABBREVIATIONS

Al_2O_3	Aluminium oxide
BN	Boron nitride
CNT	Carbon nanotube
CPU	Central Processing Unit
CuO	Copper oxide
DI	De-ionized
EG	Ethylene glycol
hBN	Hexagonal boron nitride
PVP	Polyvinylpyrrolidone
SiO_2	Silicon dioxide
TiO_2	Titanium dioxide

1. INTRODUCTION

1.1. Problem Overview

Electronic devices exist in every aspect of our daily life, from computers and mobile phones to appliances and vehicles. Also usage of these devices is escalating everyday with increasing demand to electronics. Although we use electronic devices extensively, the way of work of these devices are generally trivial to us. Generally electronic devices consist of electronic components such as transistors, resistors, transformers and capacitors require electric current to accomplish their functions.

Before the invention of transistors, vacuum tubes were used in many electronics such as television, radio and early computers. Even vacuum tubes played essential role in the beginning of electronics industry, their reliability and efficiency were very poor in comparison to their demand for space and power which was mostly wasted as heat.

A new era started in electronics industry with the invention of transistors in 1948. Few transistors, resistors, inductors and capacitors were used in the early electronic circuits which had poor performance with minor heat generation. Later on, advancements in semiconductor manufacturing led the development of the chip which is a single semiconductor piece consists of many electronic components. Different chip companies manufactured integrated circuits and larger scale integrated circuits with up to a few hundred to a few million components over the past years.

In 1970s, technological advancements had led to development of microprocessor by the Intel Corporation which was another milestone of the electronics industry. Figure 1.1. shows the number of transistors in a microprocessor, also known as central processing unit (CPU), with their introduction years. Increasing trend in the Figure 1.1. verifies the Moore's law which is named after Gordon E. Moore, who is co-founder of Intel Corporation. According to Moore's law, over the history of computing hardware, the number of transistors in a dense integrated circuit doubles approximately

every two years.

Electronic components can operate for many years safely and efficiently under the optimal operation temperatures. However, heat generation occurs when the current flow through a electronic component. Although each component generates little amount of heat individually, as the number of the components increases the amount of the heat generated gets higher and higher. This heat generation becomes enormous

Figure 1.1. Change of the transistor count in a microprocessor over the past years

for miniature electronic packages which consists of millions or even billions electronic components and heat removal becomes a necessity for reliability and safety of these electronic systems. Increasing operation temperature causes increase in the failure rate of electronic devices and without a proper cooling system failure of electronics become

inevitable as shown in Figure 1.2.

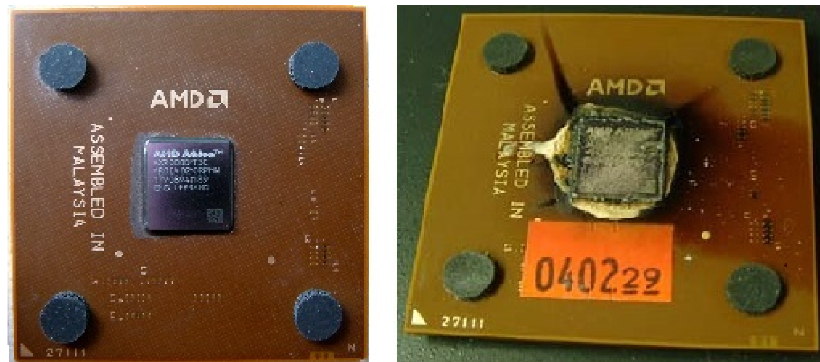

Figure 1.2. A CPU of a computer before and after overheating failure

1.2. Cooling Techniques

While generated heat in the electronic systems have been increasing with the new developments that make possible the production of miniature electronic components, different cooling methods used for thermal management of these electronics has varied widely over years. Cooling techniques for electronic devices can be classified under three categories with respect to their heat transfer rate. Figure 1.3 represents comparison of these cooling techniques for 80°C temperature difference between surface temperature and ambient temperature [1].

1.2.1. Radiation and Natural Convection Cooling

Radiation and natural convection cooling techniques do not require additional components for cooling process which makes this technique the most basic and simplest method of cooling. Radiative cooling is related to the emission of thermal radiation from the hot surface and depends on conditions of surface, temperatures of radiating surface and surroundings. Natural convection occurs energy transfer due to both bulk and molecular motion of the fluid. In this type of cooling important parameters are density of the fluid, temperature difference between surrounding fluid and surface temperature, surface dimensions and orientation. To increase the convective heat transfer extended surfaces such as heat sinks can be used in this type of cooling and these

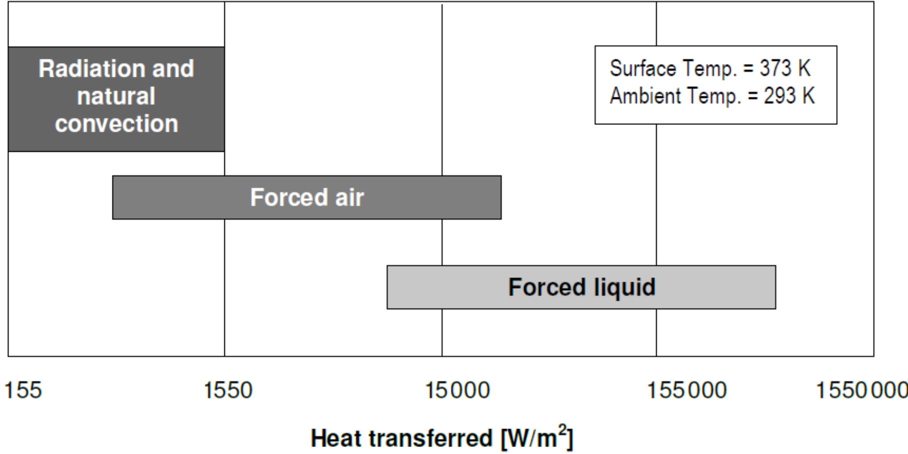

Figure 1.3. Heat transfer performance of cooling techniques

heat sinks are simply attached on surface of the electronic parts. Figure 1.4 shows some of the heat sinks with different dimensions and shape manufactured according required cooling load. This technique can be considered as simplest one but it has the lowest heat transfer capabilities among the others which is not applicable for high heat generated systems.

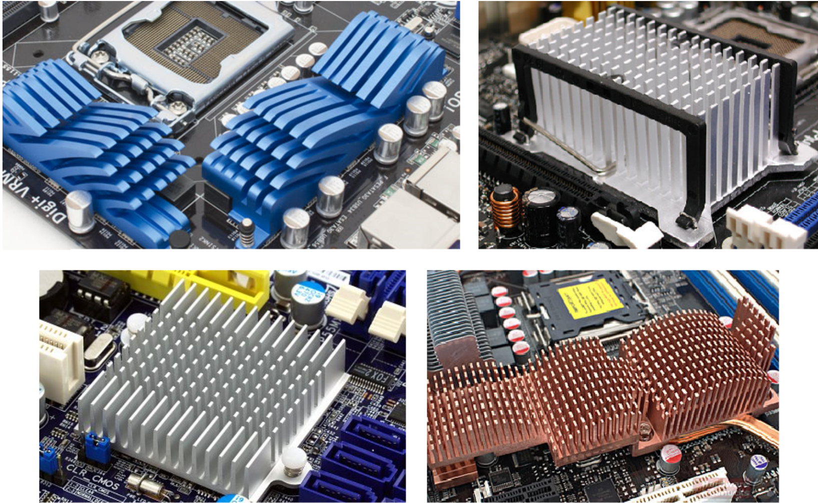

Figure 1.4. Different heat sinks used in natural convection cooling technique

1.2.2. Forced Air Cooling

Forced air cooling takes place when air flow is driven by a fan or blower. Fan is the one of the main components which is used to cool the heated surfaces in forced air cooling applications. Both forced air and natural convection cooling techniques depend on same parameters, but in the forced air cooling the velocity of air has great importance which affects the flow type. Type of the flow can be laminar or turbulent due to the features of system and the properties of air. Between these two patterns turbulent flow has the higher heat transfer rate due to existence of the chaotic patterns in the turbulence. Similar to the natural convection, heat sinks are used in forced air cooling to increase the heat transfer area. Figure 1.5 shows fan and heat sink combinations with different configurations and shapes which are manufactured for required cooling load.

Figure 1.5. Different heat sink and fan cofigurations used in forced air cooling technique

1.2.3. Forced Liquid Cooling

Although air cooling is the most widely used method for cooling electronics in computers, liquid cooling techniques are getting more popular and have been used due to high thermal conductivity of liquids. Also higher density and specific heat of liquids considerably increase their heat absorption capacity as coolants in comparison to air. The forced liquid cooling system consists of several components. Figure 1.6

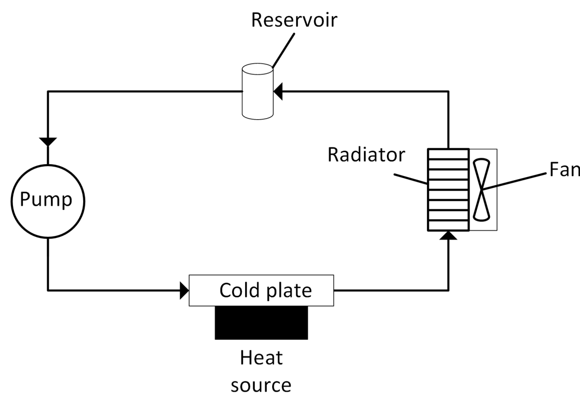

Figure 1.6. Schematic diagram of simple forced liquid cooling system

shows a simple liquid cooling system with auxiliary equipment such as a pump to circulate the liquid coolant in the system, a cold plate which is mounted on the top of the microprocessor and absorbs the generated heat from it, a reservoir and a radiator with a fan attached to it where heat exchange occurs between coolant and ambient. Commercial liquid cooling systems which are installed computer cases, are shown in Figure 1.7.

<u>1.2.3.1. Liquid Coolants.</u> There are various water and non-water based coolants that can be used in cooling systems of electronics. As mentioned before, these coolants must have high thermal conductivity, high specific heat and low viscosity. In addition to favorable thermophysical properties, they should be non-hazardous, non-flammable, non-corrosive and have a low freezing point.

Figure 1.7. Commercial liquid cooling systems

According to these criteria, de-ionized (DI) water is the most widely fluid used in cooling applicaitons. However, high freezing point of DI-water which may cause damage to the system at low temperatures, makes the DI-water impractical to use in closed loop systems. Generally, this problem can be solved by adding propylene glycol or ethylene glycol (EG) to DI-water, but it reduces the thermal conductivity and specific heat of mixture while increasing its viscosity.

Fluorinated compounds like perfluorinated polyethers, hydrofluoroethers and perfluorocarbons are some of the non-water based coolants. Although, these liquids are non-hazardous, non-flammable with a low viscosity and freezing point, their thermal conductivity and specific heat are lower compared to DI-water.

1.3. Nanofluids

Even all the features of liquid cooling have received attention, researchers have been trying to create more efficient cooling systems by using different approaches. One of them was adding micrometer- or millimeter-sized solid particles into the base fluids [2–4]. However, utilization of such liquids cause many problems in thermal applications. The main problem with liquids containing micrometer- or millimeter-sized solid particles was quick sedimentation of particles. Also, circulation of these fluids in a system caused erosion in the pipe walls and system components due to continuous and rapid strike of the particles to walls. In addition, stability problems

related to dispersed particles in base fluids might lead to clogging in channels, increase in pressure drop and pumping power requirement [5].

Choi [6] introduced the concept of nanofluids as carrier liquids containing nano-sized particles with at least one dimension less than 100 nm. Nanofluids, with their increased conductivity [7] mechanisms and higher convective heat transfer performance [8] compared conventional working fluids, are expected to be the next generation coolants in thermal engineering applications. Moreover, problems related to the suspensions of millimeter- or micrometer-sized solid particles like sedimentation, clogging and erosion of the pipe walls are not expected to occur with nanofluids due to their nano-scale dimensions.

1.4. Literature Survey

Liquid cooling of electronics have been studied to create more efficient cooling systems by using different approaches by researchers since 1960. In 1981, Tuckerman and Pease [9] introduced microchannel heat sinks in cold plates of liquid cooling systems for integrated circuits. The tested microchannel heat sink had a sink-to-inlet resistance of 0.09°C-cm^2/W. Following Tuckerman and Pease's innovative study, many researchers investigated improving the performance of liquid cooling systems using microchannel heat sinks both through numerical analysis [10–14] and experimental studies [15–19].

Another approach for improving liquid cooling system performance is through using working fluids or coolants with improved properties. While investigation of such coolants has been a continuing area of interest for chemical industry, a new class of improved working fluids, nanofluids, was introduced by Choi [6]. They have received an increasing attention by research community as they exhibit remarkable improvements compared to the base fluid properties. While some of the studies show good agreements with the predictions of effective medium theories [20, 21], others have reported anomalous increase in thermal conductivity [7, 22, 23]. Although the governing physical mechanisms behind such anomalous increase is still under debate, some of the leading mechanisms are considered to be percolation due to particle clustering [22, 24], appear-

ance of the denser liquid layer around nanoparticles known as nanolayer [24, 25], and micro convection effects due to Brownian motion of nanoparticles [26, 27]. Moreover, the effective mechanism changes for different base fluid and particle materials. Therefore, there exists no generic model to describe the change in thermophysical properties and experimental studies are required for understanding the behavior of new nanofluids.

The forced convection performance of many nanofluids are investigated by researchers under various conditions. Kumar *et al.* [28] studied on convective heat transfer and friction factor of Al_2O_3-water nanofluids in a helically coiled tube for 0.1%, 0.4% and 0.8% at Reynolds numbers between the range of 5100-8700. They observed 18% and 25% enhancement in heat transfer coefficient compared to water for 0.4% and 0.8% particle volume fractions, respectively. Zanjani *et al.* [29] investigated laminar forced convective heat transfer of water based graphene nanofluids in a circular pipe. They reported 14.2% enhancement in convective heat transfer coefficient and 10.3% enhancement in thermal conductivity by using 0.02% particle volume fraction at $Re = 1850$. Pak and Cho [30] reported an increase in Nusselt number with increasing particle volume fraction for Al_2O_3-water nanofluid at a constant Reynolds number. However, they observed a significant decrease in convective heat transfer coefficient and increase in pumping power with respect to those of pure water at a constant flow rate. Similarly, there are other studies where deterioration in thermal performance is reported. Piratheepan and Anderson [31] studied on turbulent forced convection heat transfer characteristics of water based multi-walled carbon nanotube (MWCNT) nanofluid in a straight tube and observed that using MWCNT-water nanofluids resulted in a decrease in heat transfer performance and an increase in pumping power. Similar deterioration in convective heat transfer coefficient were also reported by others [32–34]. A comprehensive review of experimental investigations of nanofluids' forced convective heat transfer characteristics is reported by Gupta *et al.* [8]. Based on the literature, there is a need for experimental data for evaluation of different nanofluids for different applications.

Many researchers investigated the cooling performance of microchannels for electronics thermal management using nanofluids as coolants. Koo and Kleinstreuer [35] numerically investigated performance of a rectangular microchannel heat-sink with nanofluids and suggested that better performance can be obtained by using working fluids having high Prandtl numbers, microchannels with high aspect ratio and high volume concentrated nanofluids. In their numerical study, Jang and Choi [36] used water based nanofluids containing 2 nm diameter diamond particles. They showed that the thermal resistance of microchannel heat sink can be reduced by 10% using nanofluid with 1% particle volume fraction, compared to using base fluid at a constant pumping power. Mital [37] showed small increase in cooling performance by using Al_2O_3-water nanofluid at constant pumping power using a semi-analytical model. Khaleduzzaman *et al.* [38] numerically examined thermal performance of water based Al_2O_3, TiO_2, and CuO nanofluids and observed decrease in thermal resistance and increase in exergy loss, pressure drop and pumping power. A review of numerical studies of nanofluid convective heat transfer is reported by Vanaki *et al.* [39].

Chein and Chuang [40] studied using CuO-water nanofluid for a microchannel heat sink experimentally. They observed that nanofluids could absorb more heat than base fluid at low flow rates, while heat transfer was dominated at higher flow rates and using nanofluids showed no improvement compared to base fluid. Ho *et al.* [41] experimentally investigated convective cooling performance of a microchannel heat sink with Al_2O_3-water nanofluid using high pumping power. They observed increase in heat transfer performance with no significant change in flow rate in spite of the increasing viscosity of nanofluid and pressure drop. Escher *et al.* [42] investigated heat transfer performance SiO_2-water nanofluid for microchannel heat sinks. They reported that increase in thermal conductivity of nanofluid should be more than increase in viscosity to achieve considerable performance enhancement. Yu and Liu [43] experimentally evaluated thermal effectiveness of Al_2O_3-water and Al_2O_3-polyalphaolefin nanofluids at constant flow rate, Reynolds number and pumping power. They concluded that overall effectiveness of nanofluids will show no improvement compared to base fluid in terms of thermal and hydrodynamic performance at constant pumping power in a liquid cooling system. Shole *et al.* [44] investigated heat transfer performance of

Al_2O_3-water nanofluid with particle volume fraction varying from 0.10% to 0.25%, by using a minichannel heat sink and reported an increase in heat transfer coefficient up to 18%. The use of the nanofluid coolants in electronics cooling systems was reviewed by Lai *et al.* [45] and they showed that nanofluids were promising coolant candidates for electronics cooling applications.

The heat transfer performance of liquid cooling systems using different nanofluids for electronics thermal management has also been studied by many researchers. Nguyen *et al.* [46] conducted experiments with a commercial cold plate using Al_2O_3-water nanofluid. They reported 40% increase in the heat transfer coefficient by using nanofluid with 6.8% particle volume fraction. They also reported that nanofluids with 36 nm particle diameter provided higher heat transfer coefficients than the nanofluids with 47 nm sized particles. Townsend and Christianson [47] built an experimental system using commercial cooling system components to investigate the heat transfer performance of Al_2O_3-water nanofluid by using a Peltier device as a heat source. They found slight increase in Nusselt number with increasing Reynolds number and particle volume fraction. Roberts and Walker [48] used a commercial liquid cooling system in their experiments and reported 20% reduction in cold plate thermal resistance by using Al_2O_3-water nanofluid with 1% particle volume fraction. However, they did not report the total system performance in their study. Putra *et al.* [49] used Al_2O_3-water and TiO_2-water nanofluids as working fluids in a heat pipe liquid-block combined with thermoelectric cooling. Their experimental results showed better performance for central processing unit (CPU) cooling by using liquid-block and thermoelectric together. Rafati *et al.* [50] investigated the performance of SiO_2, TiO_2 and Al_2O_3 nanofluids with a commercial liquid cooling kit and used 75% water and 25% of ethylene glycol (EG) mixture as base fluid. The best results were observed for Al_2O_3 nanofluid with 1% particle volume fraction. In their experimental study Selvakumar and Suresh [51] used a copper cold plate to investigate convection performance of CuO-water nanofluid and obtained 30% increase in heat transfer coefficient for 0.2% particle volume concentration. Nazari *et al.* [52] worked with Al_2O_3 and carbon nanotubes (CNT) to investigate CPU cooling performance of nanofluids. Their results showed 20% and 22% reduction in junction temperature for 0.5% Al_2O_3-water nanofluid and 0.25% CNTs-water

nanofluid at 21 mL/s flow rate, respectively.

Hexagonal boron nitride (hBN), the softest form of polymorphs of boron nitride (BN), and recently introduced hBN nanofluids can be considered as one of the most promising coolant candidates for liquid cooling applications due to their superior thermal characteristics. Since their recent introduction, only a few studies report about their thermophysical properties and stability. Li *et al.* [53] used 70 and 140 nm sized BN particles to investigate thermal conductivity enhancement of BN-EG nanofluids and reported that specific surface area and aspect ratio of nanoparticles could be the main reasons for abnormal difference between thermal conductivity enhancements. Guo *et al.* [54] studied on BN-EG nanofluids with different surfactant materials. They observed improvement both in stability and fluidity of nanofluid by using poly-vinyl-pyrrolidone (PVP) with a slight decrease in thermal conductivity. İlhan *et al.* [55] experimentally investigated heat transfer enhancement and viscosity change of hBN nanofluids with particle volume concentration varying between 0.03% and 3% using DI water, EG, EG–DI water mixture as base fluids. They reported significant thermal conductivity increase even with dilute volume concentrations compared to the viscosity increase. There exist limited studies in regards to convection heat transfer performance of hBN nanofluids. İlhan and Erturk [56] investigated the convection performance of hBN-water nanofluids for a circular tube subject to uniform heat flux with laminar, thermally developing flow and reported that the increase in the convection heat transfer coefficient is proportional to that of thermal conductivity.

1.5. Objective

Recent studies have shown that there are potential benefits of using hBN nanofluids as next generation coolants for various thermal engineering applications due to their remarkable thermophysical properties. However, there are relatively limited studies in literature related to BN or hBN nanofluids, and further investigations are needed for identifying their performance for various thermal applications such as cooling of electronics. This study aims to identify the potential benefits of using hBN nanofluids for electronics cooling. Therefore, cooling performance of hBN nanofluids are investigated

by using two experimental liquid cooling systems. Two different cold plates are used in the first experimental system to obverse convective heat transfer behavior of nanofluids at constant flow rates. An instrumented commercial closed loop liquid cooling system is used as the second experimental system, where the performance is examined subject to a pump performance curve constraint.

2. METHODOLOGY

2.1. Experimental Procedure

2.1.1. Nanofluid Preparation

As the first step of experimental procedure, preparation of nanofluids used in the experiments are done by using two step method. Two different nanofluids, hBN-water with 0.1%, 0.5%, 1%, 2% volume concentration and Al_2O_3-water with 0.5% volume concentration, are prepared and DI-water is used as base fluid in all prepared nanofluids.

hBN nanoparticles with 70 nm average particle size, purchased from MK Impex Corp. (purity: 99.5%, density: 2.23 g/cm^3), are used in the hBN-water nanofluids preparation. Poly-vinyl-pyrolidone (PVP K30) surfactant material is used to increase stability of hBN-water samples with different weight concentrations according to volume concentration of nanofluids. 0.1% and 0.5% volume concentrated hBN nanofluids are prepared with 0.05% weight concentrated surfactant and 1%, 2% volume concentrated hBN nanofluids are prepared with 0.1% weight concentrated surfactant. Required amount of surfactant material, weighed with a precision balance (Kern, PFB 200-3), is introduced to base fluid and stirred using a mechanical homogenizer (Heidolph, RZR 2021) for ~15 minutes at ~1500 rpm. Following that, required amount of hBN nanoparticles are introduced to homogenous surfactant-base fluid solution and stirred for ~45 minutes at ~1500 rpm. After the mechanical mixing process, nanoparticle containing mixture is placed into ultrasonicator (Hielscher UP400S with sonotrode H22) and sonicated for ~2 hours at ~160-180 W power. During the ultrasonication process nanofluid sample is placed into a temperature controlled water bath (PolyScience 9106A12E) to eliminate evaporation and prevent excessive heating of sample. Detailed information about preparation of hBN-water nanofluids and characterization of hBN nanoparticles are presented by İlhan *et al.* [55].

Al_2O_3-water nanofluids are also prepared with two step method by following same procedure as in the hBN nanofluid preparation without using surfactant material. Weighted Al_2O_3-gamma nanoparticles, with 15 nm average particle size (MK Impex Corp., purity: 99.5%, density: 3.89 g/cm^3), are introduced to DI-water and stirred by a mechanical homogenizer for ~45 min at 1500 rpm. After that, prepared suspension is placed into the ultrasonicator and sonicated with ~160-180 W power for ~ 2 hours. Details of nanofluid preparation is summarized in 2.1.

Table 2.1. Details of nanofluid preparation.

<table>
<tr><th>Nanofluid</th><th>Concentration [% by volume]</th><th>Ultrasonication time [hour]</th><th>Surfactant</th><th>Surfactant [% by weight]</th></tr>
<tr><td rowspan="2">hBN-water</td><td>0.1, 0.5</td><td rowspan="2">2</td><td rowspan="2">PVP</td><td>0.05</td></tr>
<tr><td>1, 2</td><td>0.1</td></tr>
<tr><td>Al_2O_3-water</td><td>0.5</td><td>2</td><td>-</td><td>-</td></tr>
</table>

2.1.2. Thermal Conductivity Measurement

Thermal conductivities of prepared nanofluids are measured with thermal property analyzer (KD2Pro, Decagon) and measurement uncertainty of device calculated as ±3% of the measured value. Measurements are conducted at 25°C right after the nanofluids are prepared and KS-1 thermal conductivity probe of the device is used. Measurement device is used in low power mode to reduce uncertainty and KS-1 probe is immersed into fluid completely. Before the nanofluid measurements, a proper validation study is conducted with DI-water and EG and it is seen that thermal conductivity results are in good agreement with the ones in literature. During the measurements, nanofluid sample in a vial is placed into a water bath whose temperature is controlled with circulating chiller (PolyScience, 9106A12E) to achieve stable thermal conditions. To prevent the environmental errors that can be caused by vibration and free convection, all the doors and windows are kept closed and all other vibrating machinery in the room are turned off including circulating water bath.

2.1.3. Viscosity Measurements

Prepared nanofluid viscosities are measured by using a programmable cone plate rheometer (Brookfield DV-III Ultra) at 25°C. The temperature of the samples is controlled by using a circulating chiller (PolyScience, 9106A12E) connected to sample cup of the rheometer. Before every measurement, rheometer is calibrated with DI-water and EG at specified temperatures with proper spindle (CP40) of the rheometer and results are validated with respect to the literature. The measurement uncertainties change with the current viscosity of the sample and the maximum device error is 0.1% of the measured value.

2.1.4. Experimental Systems

Two different liquid cooling systems are used in this studyto test the performance of hBN-water nanofluids in this study together with 0.5% Al2O3-water nanofluid to provide a reference. The first experimental system is assembled by using several liquid cooling components, whereas a commercial liquid cooling system is used as the second experimental system. Water based hBN and Al_2O_3 nanofluids are prepared by using the two-step method using ultrasonication and surface active material is used in preparation of hBN nanofluids to achieve stability. Thermal conductivity and viscosity of nanofluids are measured before and after the experiments to monitor any change. Details of experimental conditions are summarized in 2.2.

Table 2.2. Details of experimental conditions.

<table>
<tr><th></th><th>Cold plate type</th><th>Flow rate</th><th>Heat load</th></tr>
<tr><td rowspan="2">First experimental system</td><td>Flat</td><td rowspan="2">Constant flow rate (0.3 - 2 L/min)</td><td>110 W</td></tr>
<tr><td>Finned</td><td>140 W</td></tr>
<tr><td>Second experimental system</td><td>Zalman LQ310</td><td>Constant pumping power</td><td>140 W</td></tr>
</table>

<u>2.1.4.1. First Experimental System.</u> First experimental liquid cooling system consists of a reservoir, a flow meter, a pump, a heat exchanger and a cold plate connected via silicon tubing with 6 mm inner diameter and brass connectors as shown in in Figure 2.1. Schematic diagram of first experimental system is provided in Figure 2.2.

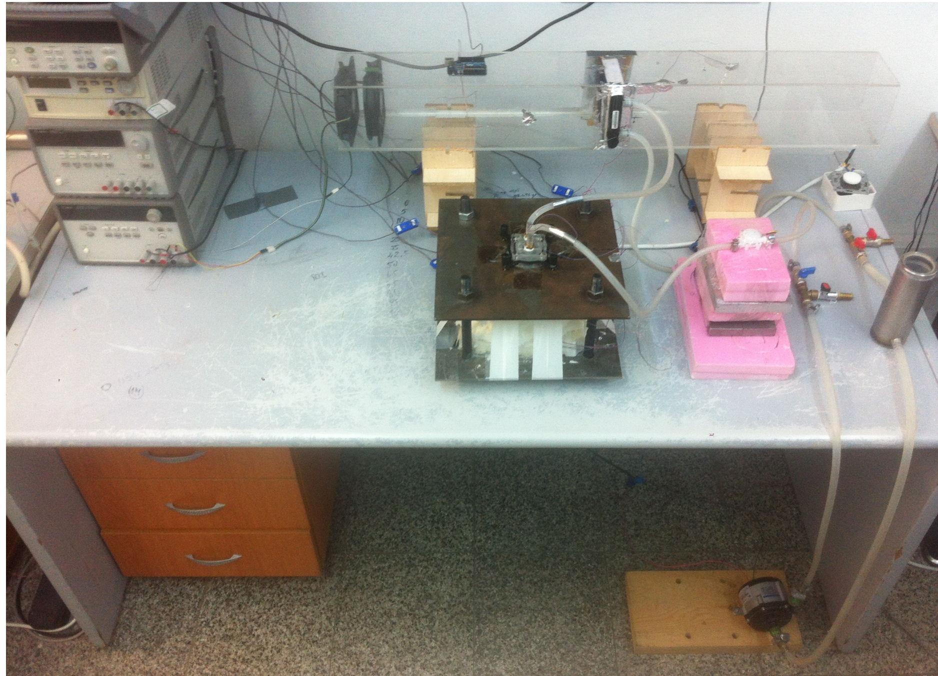

Figure 2.1. First experimental system

A heater block is designed and manufactured from copper as a one-piece by using lathe and milling machine to simulate the behavior of a CPU of a computer as shown in Figure 2.3.

A commercial software (ANSYS) is used to determine the dimensions of heater block and the temperature distribution is shown in Figure 2.4. Technical drawing of manufactured heater is provided in Appendix A.

The heater block is comprised of three sections; the body (20 mm x 50 mm x 70 mm height), the neck (10 mm x 10 mm x 40 mm height) that resembles the uniformly powered die and the lid (30 mm x 30 mm x 2 mm thickness) resembles the lid of the package as shown in Figure 2.5. The heater is designed to provide a uniform heat

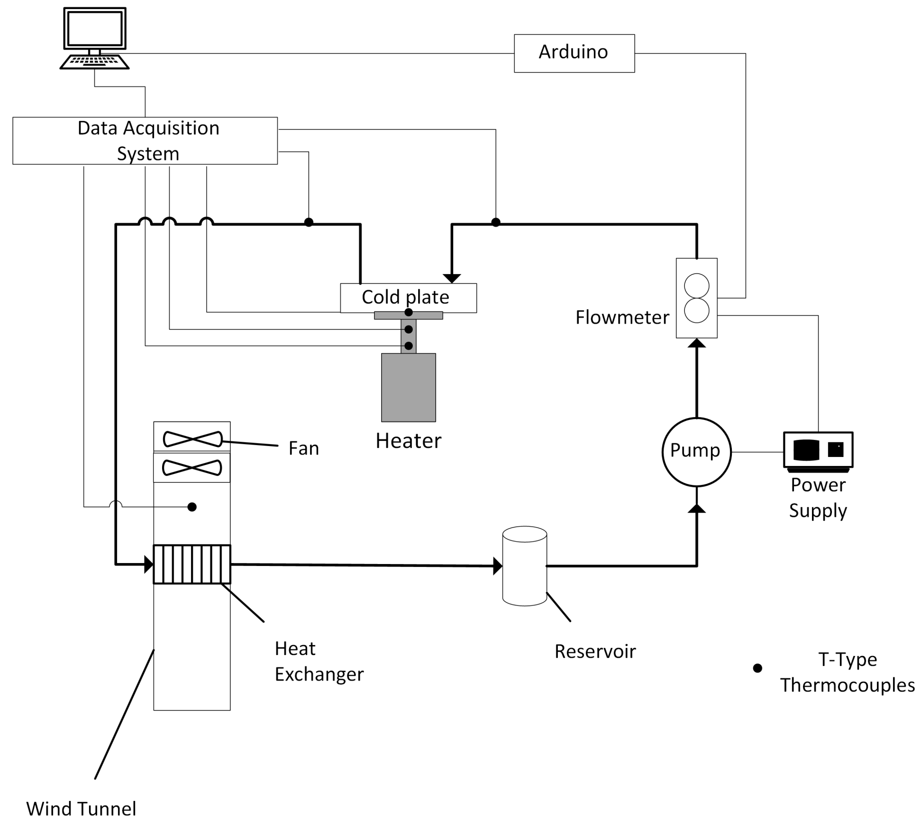

Figure 2.2. Schematic diagram of first experimental system

Figure 2.3. Copper heater block

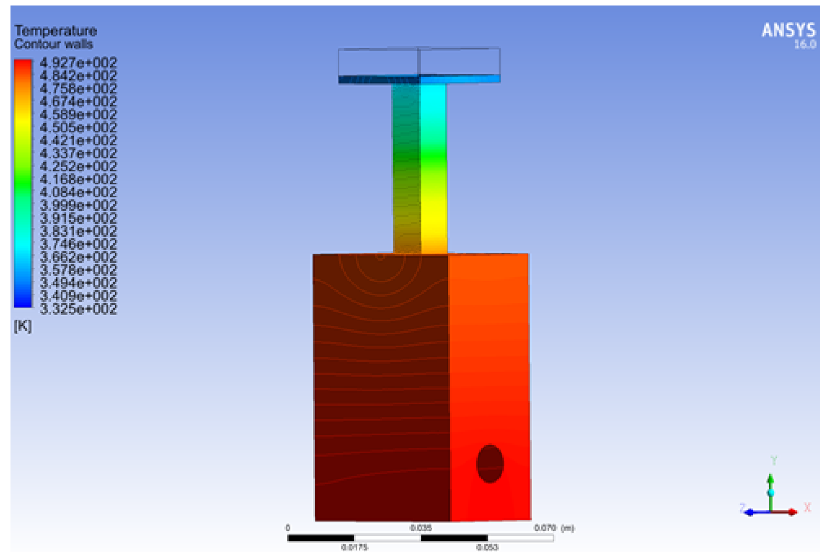

Figure 2.4. Temperature distribution in heater block

through the neck section to represent the equivalent thermal behavior of test chips that are known as thermal test vehicles. A 40 mm long cartridge heater of 10 mm diameter is that can be heated up to 220W is embedded into the body. Two 36 AWG thermocouples, T_{h1} and T_{h2} are attached to center of the neck through two holes, 80 mm and 100 mm from the bottom of heater, to calculate the heat flux through the neck. The heat spreads through the lid that resembles the integrated heat spreader of a CPU package. Another thermocouple is attached to the lid through a groove to measure the case temperature, T_c. The heater block assembly is carefully insulated with glass wool, ceramic fiber board and ceramic fiber blanket to minimize heat loss during all experiments.

Two different cold plates are used in the experiments of first experimental system. First cold plate (Bykski, CPU-XPH-B) has finned surface of size 36 x 23.5 mm with a jet plate over it made from nickel plated copper shown in Figure 2.6. Fin depth, fin thickness and spacing between two fins are measured as 1 mm, 0.5 mm and 0.48 mm, respectively. The second one (i-Tech) is a flat cold plate that has a circular heat transfer area with 20 mm diameter, also made of copper as seen in Figure 2.7. During the experiments, the cold plate is mounted on the top of the heater by using a torque

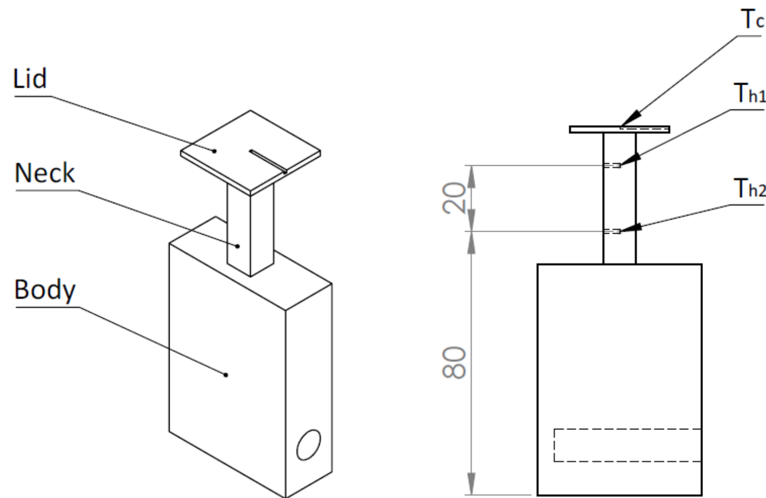

Figure 2.5. Sections of heater block and locations of thermocouples

wrench to ensure uniform pressure through all connections. A thin film of a thermal interface material is applied between the lid and the cold plate base to minimize thermal contact resistance.

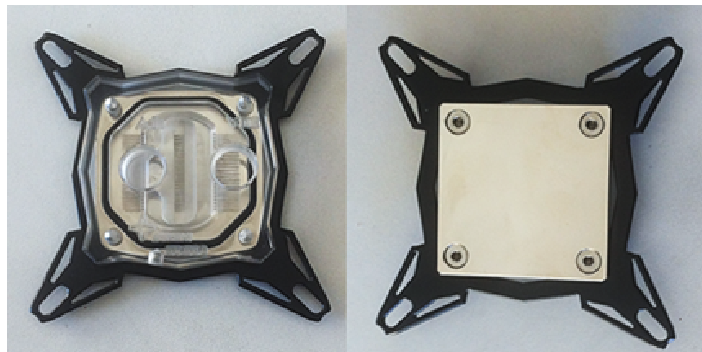

Figure 2.6. Finned cold plate

Two T-type thermocouples are installed at the inlet and exit of the cold plate, T_i and T_o. These thermocouples are inserted into the connector tubes, right after the flow meter and cold plate exit, before the flow develops so that the measurements resemble the mean fluid temperature accurately. Another thermocouple is used to measure to ambient air temperature, T_a, at the inlet of the wind tunnel. A single row, two pass, cross-flow aluminum heat exchanger with overall dimensions of 12 x 12 x 2.5 cm is used in the first experimental system. The heat exchanger is mounted to a wind

tunnel manufactured from acrylic glass with the dimensions of 12 x 12 x 110 cm as shown in Figure 2.8.

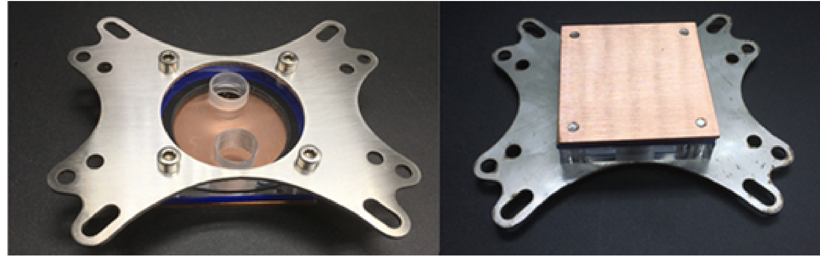

Figure 2.7. Flat cold plate

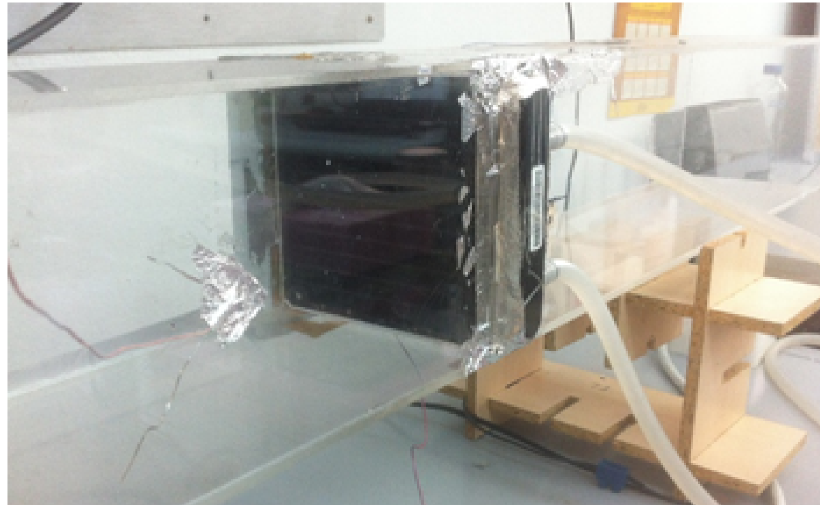

Figure 2.8. Heat exchanger mounted in the middle of wind tunnel

Two fans (Zalman ZP1225ALM) are attached to one end of the wind tunnel that are capable of providing 2851.2 L/min (100.6 ft^3/min) air flow to the heat exchanger with 12 V applied. To calculate air flow rate, cross section area of the wind tunnel is divided into elementary surface elements to measure the air velocity in each of them and then average air velocity weighted over the surfaces is calculated. The air flow rate is then calculated by multiplying mean air velocity and cross section area of the wind tunnel and measured by using an anemometer (Airflow TA-2).

The laboratory ambient temperature is kept constant at 25°C during all experiments. All thermocouples used in the study are T-type (Omega Inc. $\sigma_T = \pm 0.5°C$)

and calibrated with a temperature controlled water bath before being installed to experimental setup. Fluid flow is provided by a centrifugal pump (Iwaki RD-20) and measured by a turbine flow meter (($\sigma_{\dot{V}}$=1% of the reading). Flow rates are adjusted with a valve, and varies from 0.3 to 2 L/min during the experiments of first experimental system. After the system reaches steady state, a data acquisition system (Agilent 34970A) is used to record temperature readings.

2.1.4.2. Second Experimental System. A commercial liquid cooling system (Zalman LQ310) is instrumented as the second experimental system without any alteration but a small acrylic reservoir to fill the system with test liquids. Copper cold plate of this system has very dense finned configuration over 33 mm x 28 mm area as shown in Figure 2.9.

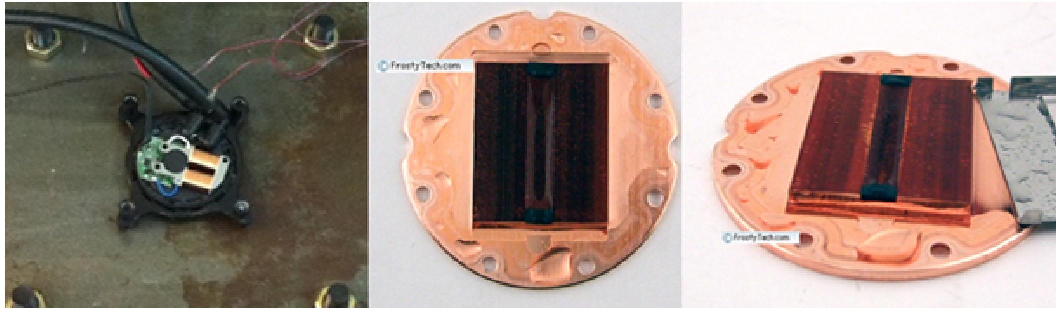

Figure 2.9. Commercial cold plate

This system has an integrated pump attached to the cold plate and experimental system and its schematic diagram is shown in Figures 2.10 and 2.11. Six T-type thermocouples (Omega Inc. $\sigma_T = \pm 0.5°C$) are mounted to the corresponding locations as mentioned for the first experimental setup. 12 V voltage is applied to the pump of the commercial liquid cooling. Both experimental liquid cooling systems are cleaned with pressurized water before and after each experiment to prevent any possible contamination.

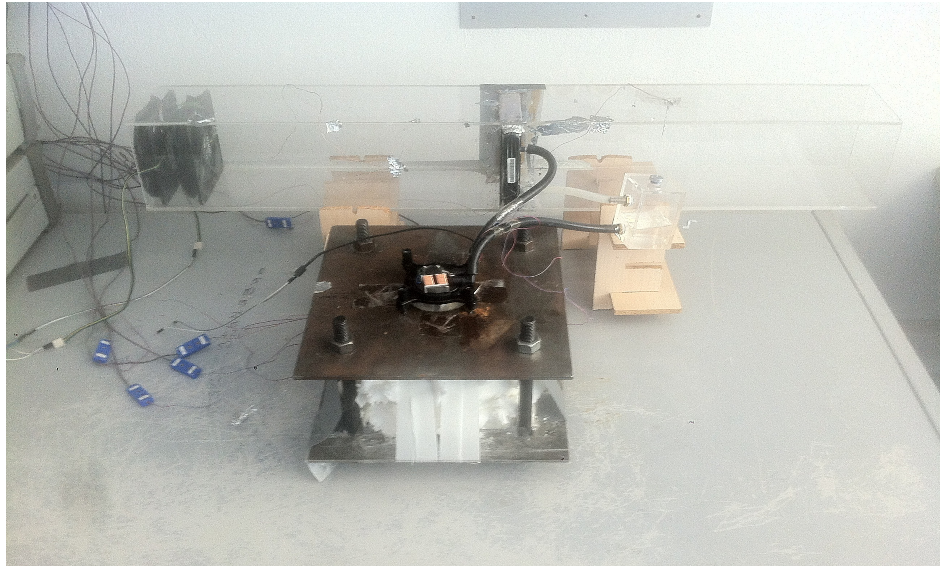

Figure 2.10. Second experimental system

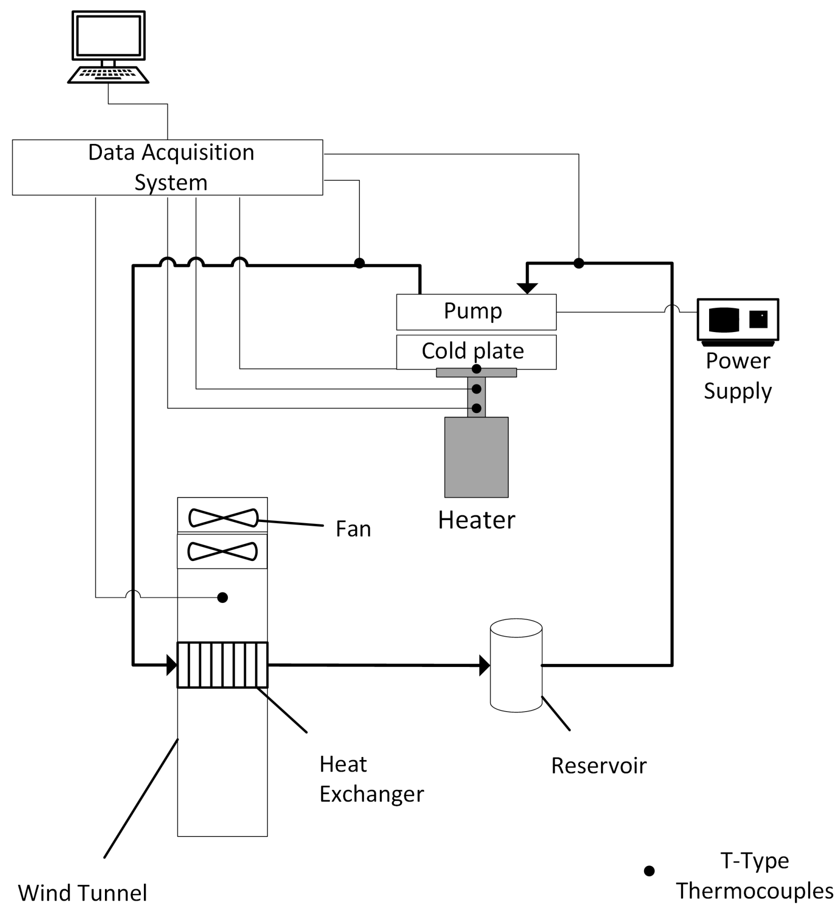

Figure 2.11. Schematic diagram of second experimental system

2.1.5. Data Analysis

Thermal resistance is the most widely used performance metric for cooling applications and it is used in this study to evaluate different nanofluids performance. Case-to-ambient thermal resistance of a CPU liquid cooling system is defined as;

$$\theta_{c-a} = \theta_{c-i} + \theta_{i-o} + \theta_{o-a} = \frac{T_c - T_a}{q} \tag{2.1}$$

where θ_{c-i}, θ_{i-o} and θ_{o-a} are cold plate, flow and heat exchanger thermal resistances, respectively and they can be defined as;

$$\theta_{c-i} = \frac{T_c - T_i}{q} \tag{2.2}$$

$$\theta_{i-o} = \frac{T_i - T_o}{q} \tag{2.3}$$

$$\theta_{o-a} = \frac{T_o - T_a}{q} \tag{2.4}$$

The thermal design power of CPU or heat load dissipated by the heater, q, is calculated from the temperatures measured from the neck section of the heater and defined as;

$$q = kA_{neck}\frac{T_{h2} - T_{h1}}{\Delta x} \tag{2.5}$$

where k, A_{neck} and Δx are the thermal conductivity of the copper which is material that heater manufactured from, the cross section area of the neck section and distance between the thermocouples respectively.

Volume flow rate of second experimental system is not measured in order not to interfere with the flow and system performance. Instead it is calculated by;

$$\dot{V} = \frac{q}{\rho c_p (T_o - T_i)} \tag{2.6}$$

Stanton number is defined as;

$$St = \frac{UA}{\dot{V} \rho c_p} \tag{2.7}$$

where overall heat transfer coefficient, U, times heat transfer area, A, is calculated as;

$$UA = \frac{q}{\Delta T_{lm}} \tag{2.8}$$

and ΔT_{lm} is log-mean temperature and it is defined as;

$$\Delta T_{lm} = \frac{T_o - T_i}{\ln(\frac{T_c - T_i}{T_c - T_o})} \tag{2.9}$$

The cooling performance enhancement is defined as;

$$E = \frac{\theta_{bf} - \theta_{nf}}{\theta_{bf}} \tag{2.10}$$

Simple mixture rule is used to calculate density, ρ_{nf}, and the specific heat, c_{nf}, of the nanofluids and presented in Equations 2.11 and 2.12.

$$\rho_{nf} = (1 - \varphi)\rho_{bf} + \varphi \rho_p \tag{2.11}$$

$$c_{nf} = \frac{(1 - \varphi)\rho_{bf} c_{p,bf} + \varphi \rho_p c_{p,p}}{\rho_{nf}} \tag{2.12}$$

Subscripts *p*, *bf* and *nf* denote quantities related to particle, nanofluid and base fluid, respectively and φ is the particle volume fraction of the nanofluid.

2.1.5.1. Experimental Uncertainties. Single sample measurement uncertainty analysis as defined by Kline and McClintock [57] is used to determine the uncertainties associated with the measurement systems. The uncertainty of heat transfer rate is defined as;

$$\sigma_q = \left[\left(\frac{\partial q}{\partial T_{h2}} \sigma_T \right)^2 + \left(\frac{\partial q}{\partial T_{h1}} \sigma_T \right)^2 + \left(\frac{\partial q}{\partial \Delta x} \sigma_x \right)^2 \right]^{1/2} \tag{2.13}$$

where σ_x is the measurement uncertainty of caliper.

Uncertainty of case-to-ambient thermal resistance can then be defined as;

$$\sigma_{\theta_{c-a}} = \left[\left(\frac{\partial \theta_{c-a}}{\partial T_c} \sigma_T \right)^2 + \left(\frac{\partial \theta_{c-a}}{\partial T_a} \sigma_T \right)^2 + \left(\frac{\partial \theta_{c-a}}{\partial q} \sigma_q \right)^2 \right]^{1/2} \tag{2.14}$$

The uncertainties of all the other reported thermal resistances can be defined similarly.

3. EXPERIMENTS AND RESULTS

3.1. Thermal Conductivity and Viscosity of Nanofluids

Nanofluids are prepared following the procedure in the previous sections and their properties are measured before and after their use in the experimental setups. The thermal conductivity and viscosity change with respect to particle volume fraction measured before the experiments are presented in Figure 3.1. It can be observed that the nanofluid to base fluid conductivity ratio exceeds that of viscosity for hBN nanofluids, whereas it is opposite for Al_2O_3 nanofluid. Similar property measurement results were reported by [55] for hBN nanofluids and [30, 58] for Al_2O_3 nanofluids.

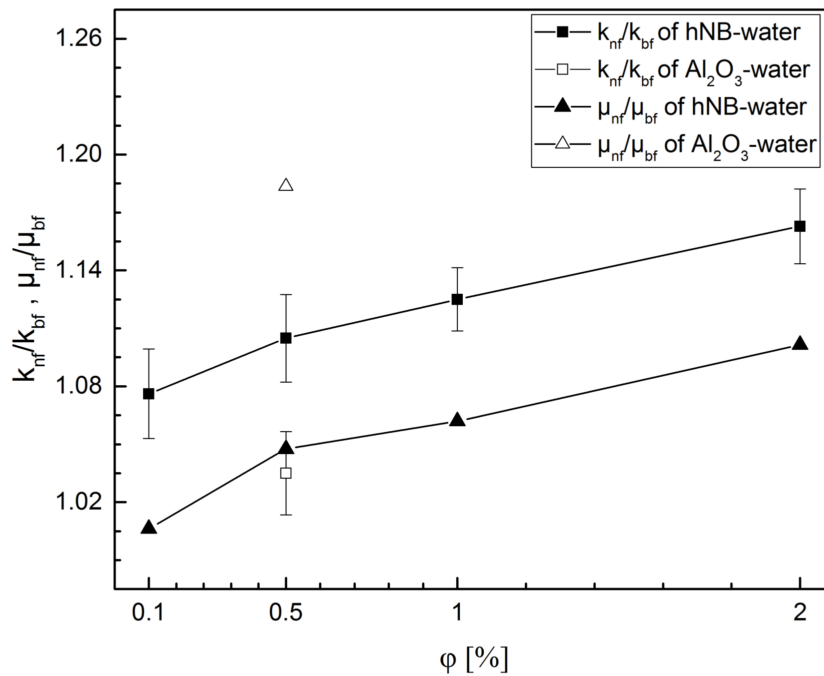

Figure 3.1. The change in nanofluid to base fluid viscosity and thermal conductivity ratios of Al_2O_3 and hBN nanofluids

The thermal conductivity increase is approximately 7.6, 10, 12.5, 16.2% and viscosity increase is 0.6, 4.7, 6.1, 10% for hBN-water nanofluids compared to base fluid for particle volume fractions of 0.1, 0.5, 1 and 2%, respectively. Al_2O_3-water nanofluid's thermal conductivity and viscosity increase are measured as 3.5% and 18.3%, respectively. No property change is observed after the experiments, showing that there was no significant particle accumulation or contamination within the experimental systems. However, the systems are still cleansed after each nanofluid experiment as explained earlier.

3.2. Experimental Results

DI-water measurements are used as a baseline and nanofluids' performance improvements are evaluated based on these measurements for both experimental systems. After the experiments with DI-water, systematic experiments are conducted with hBN-water nanofluids with different particle volume fractions. Experiments for first experimental system are conducted at flow rates varying between 0.3 L/min and 2 L/min with flat and finned cold plates. Heat loads used in the experiments are 110 W for flat cold plate experiments and 140 W for finned and commercial system experiments. All experiments in this study are repeated three times and it is seen that data collected in all these experiments were within the mean value which is beyond the limits of measurement uncertainty.

3.2.1. Results of First Experimental System

Case-to-ambient thermal resistance change of system with flat cold plate are presented in Figure 3.2. The thermal resistance of the system decreases with increasing volume concentration of hBN-water nanofluids while results of Al_2O_3-water nanofluid showed no measurable change with respect to base fluid. The enhancement in case-to-ambient thermal resistance is approximately 4, 6.8, 8.1, 11.2% for hBN-water nanofluids for particle volume fractions of 0.1, 0.5, 1 and 2%, respectively. It can be observed that the performance improvement achieved by introducing 0.1% hBN particles is similar to that achieved by increasing particle volume fraction from 0.1% to 1%. Therefore, there

is a diminishing improvement achieved by increasing particle volume fraction that is consistent with results reported in [55] and [56].

Similar to case-to-ambient thermal resistance, thermal resistances of cold plate and heat exchanger have analogous decreasing trend for hBN-water nanofluids as seen in Figure 3.3 and Figure 3.4. The thermal resistance decreases approximately by 4, 6.8, 8.5, 11.8% for flat cold plate and 3.7, 7, 8.1, 11.3% for heat exchanger for hBN particle volume fractions of 0.1, 0.5, 1 and 2%, respectively. Although similar reduc-

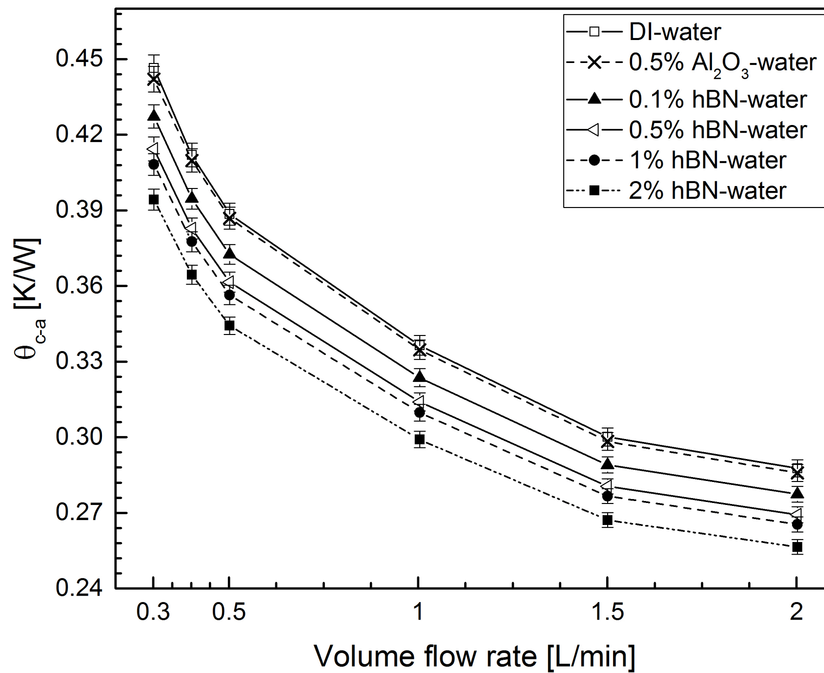

Figure 3.2. The change in case-to-ambient thermal resistance of first experimental system with flat cold plate

tion percentages are obtained for thermal resistances of cold plate and heat exchanger, thermal resistance of cold plate comprises more than %80 of case-to-ambient thermal resistance. Therefore reduction in cold plate thermal resistance has greater effect compared to thermal resistance of heat exchanger.

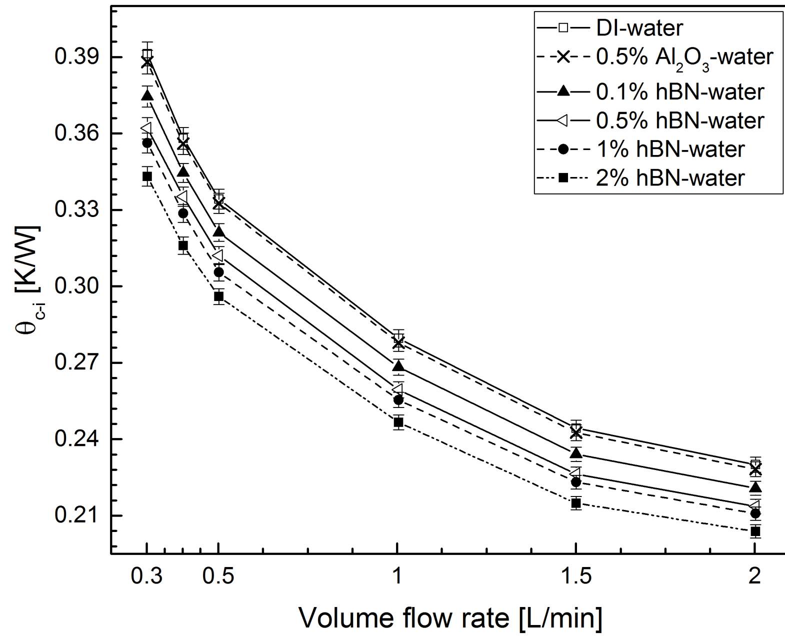

Figure 3.3. The change in thermal resistance of flat cold plate

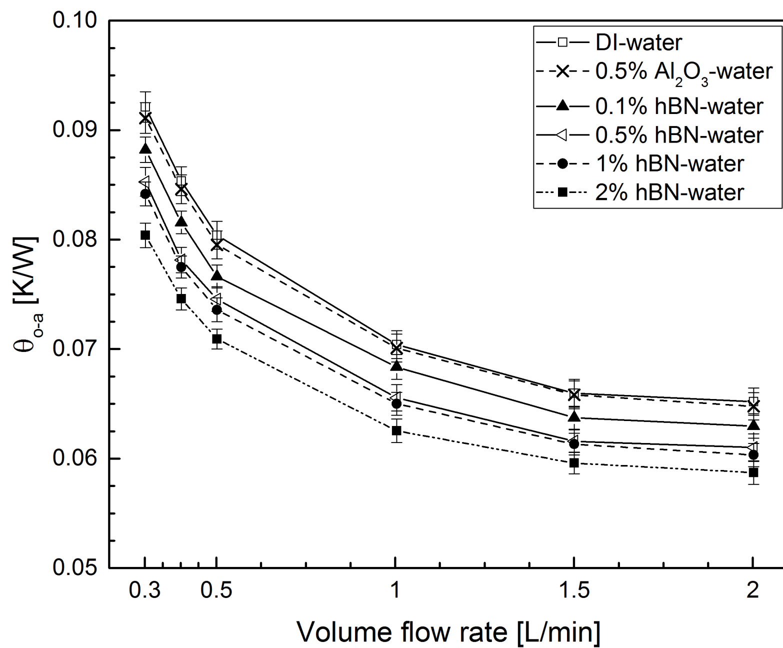

Figure 3.4. The change in heat exchanger thermal resistance of first experimental system with flat cold plate

At the second part of the experiments with first experimental system, finned cold plate is used as described in previous sections. Similar trends in thermal resistances are observed while Al_2O_3-water nanofluid results showed no significant deviation from that of DI-water. Using the finned cold plate significantly improves the case-to-ambient and cold plate thermal resistances compared to those for flat cold plate as can be observed in Figure 3.5 and Figure 3.6. As a result, the achieved heat transfer enhancement rate by using nanofluids reduce for the finned cold plate experiments. The measured heat

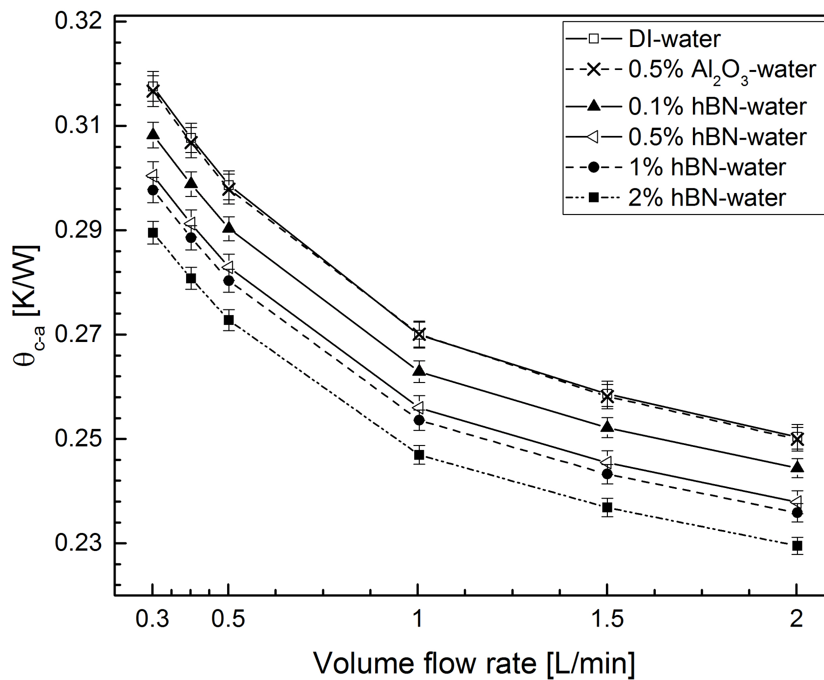

Figure 3.5. The change in case-to-ambient thermal resistance of first experimental system with finned cold plate

exchanger thermal resistance for experiments with finned cold plate is observed to be very similar to experiments with flat cold plate and presented in 3.7. The decrease in thermal resistance for finned cold plate experiments are observed to be 2.4, 4.7, 5.5, 7.8% for the case-to-ambient, 2.3, 4.9, 5.5, 8% for finned cold plate for hBN particle volume fractions of 0.1, 0.5, 1 and 2%, respectively.

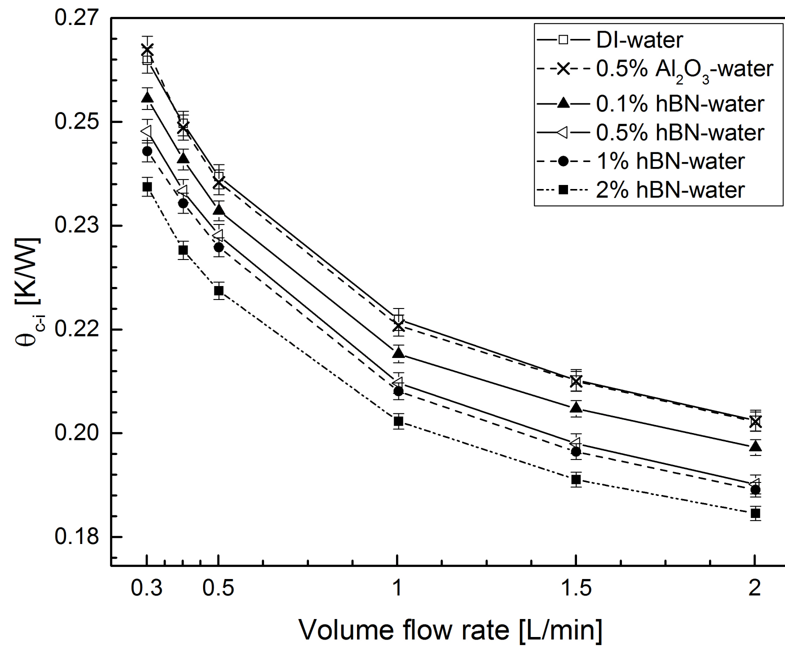

Figure 3.6. The change in thermal resistance of finned cold plate

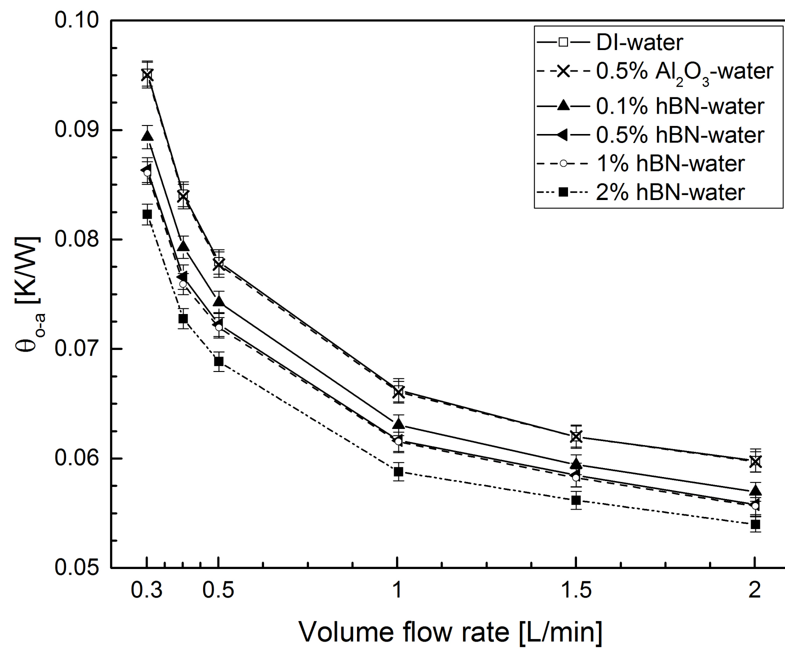

Figure 3.7. The change in heat exchanger thermal resistance of first experimental system with finned cold plate

The experiments show that the use of hBN improves thermal performance especially for systems that are limited with convection rates due to limited heat transfer area. Whereas, the tested Al_2O_3 nanofluid does not exhibit any performance improvement. Moreover, diminishing improvements are observed with increasing hBN particle volume fraction. However, it must be stated that the observed increase by using hBN nanofluids is optimistic. Although the thermal resistances of the system decrease with increasing hBN particle loading for constant flow rates, the expected decrease in volume flow rates due to increasing viscosity and pressure drop is not accounted in the results.

3.3. Results of Second Experimental System

An additional set of experiments are carried out to identify the effects of increasing viscosity and pressure drop. A commercial computer liquid cooling system is instrumented as the second experimental system and hBN-water and Al_2O_3-water nanofluids with same volume concentrations used in the set of experiments are tested. The pump of the commercial cooling system is operated at a constant power, and the effect of increased viscosity can be observed in these experiments. Therefore, each nanofluid is tested for a unique flow rate, the operating flow rate for that particular nanofluid, and the measured thermal resistances represent the performance at the operating flow rate of the particular working fluid.

The results of the experiments with commercial system are presented in Figures 3.8, 3.9, 3.10. Also effect of different particle volume fractions of nanofluids on case-to-ambient and cold plate thermal resistances are presented in 3.11. Similar to the results of first experimental system, thermal resistances decrease with increasing hBN particle volume fraction, despite the reduction in the operating flow rate. Moreover, the measured cold plate thermal resistance is smaller for the commercial system as the cold plate of the commercial cooling system has a denser fin configuration than the ones used in first experimental system.

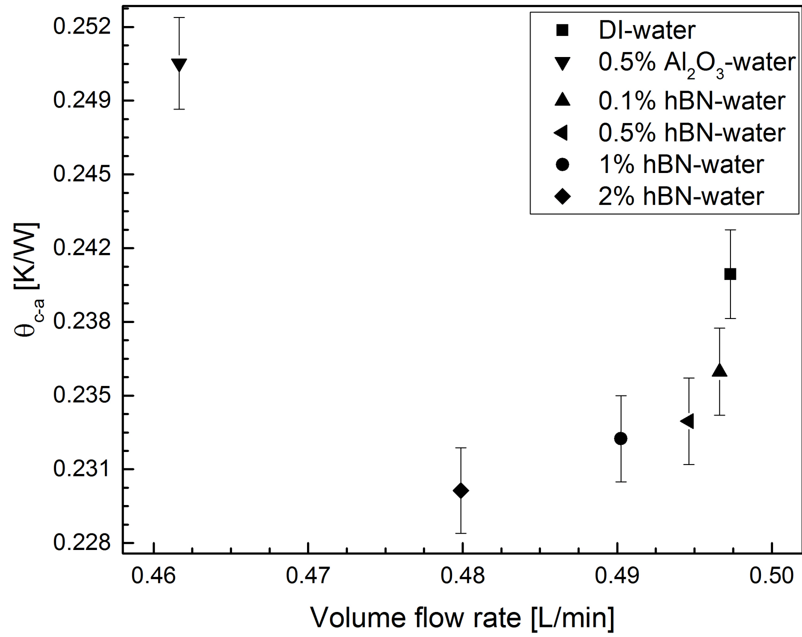

Figure 3.8. The change in case-to-ambient thermal resistance of second experimental system

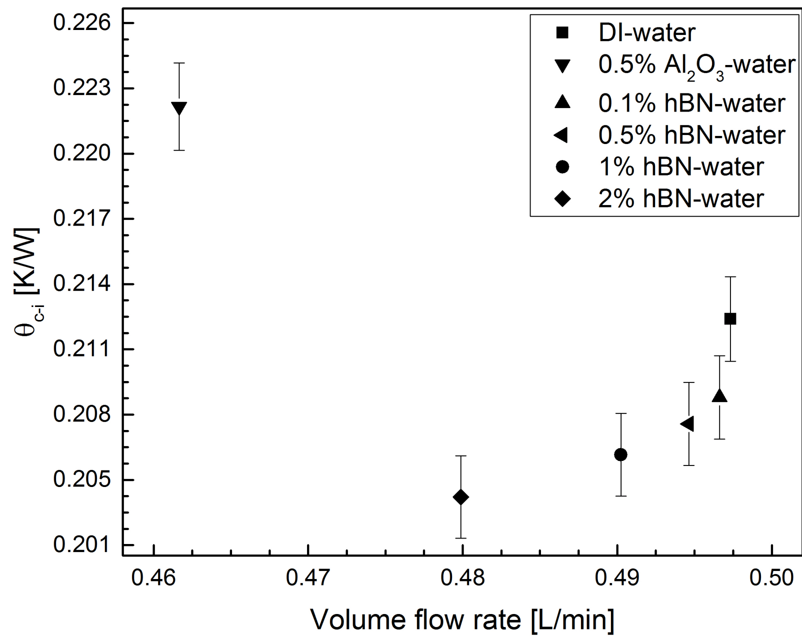

Figure 3.9. The change in cold plate thermal resistance of second experimental system

Despite the decreased flow rates with increasing hBN particle loading, the maximum enhancement in thermal resistance reduction is obtained by using hBN-water nanofluid with 2% particle volume fraction and it is calculated as 4.3, 4, and 5.5% for the case-to-ambient, cold plate and heat exchanger, respectively.

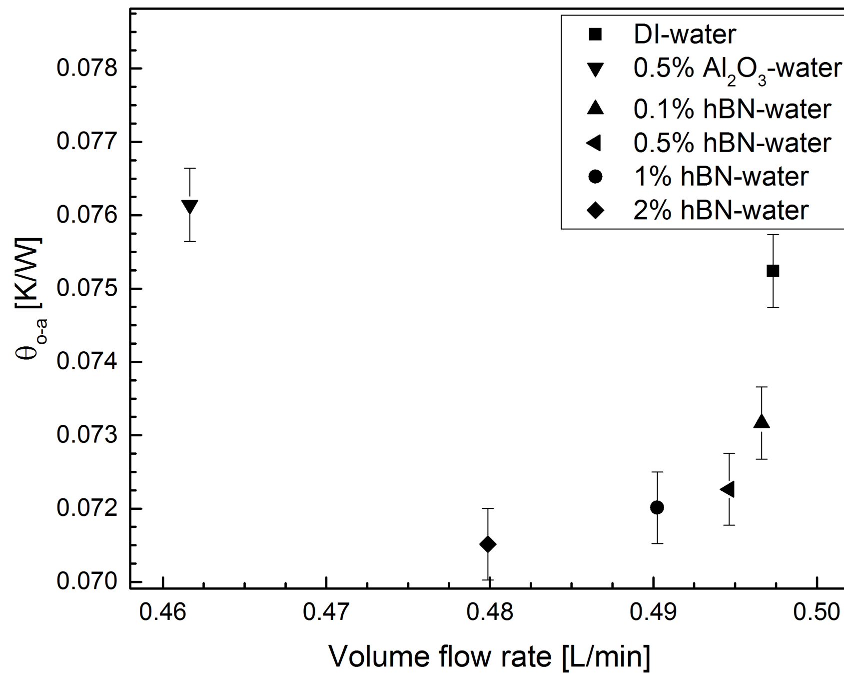

Figure 3.10. The change in heat exchanger thermal resistance of second experimental system

In contrast to hBN-water nanofluid, results for Al_2O_3-water nanofluid experiments with pumping power constraint showed an increase in thermal resistance with respect to base fluid as presented in figures above. The increase in thermal resistance for Al_2O_3-water nanofluid is related to the significant decrease in the flow rate due to high viscosity, and relatively lower increase in conductivity as presented in Figure 3.1. It is clear that thermal conductivity increase should exceed the viscosity increase to achieve thermal resistance improvement in commercial cooling system. This observation is consistent with the findings of Escher *et al.* [42] as a result of their experiments with SiO_2 nanofluids. Besides, Townsend and Christianson [47] observed an increase

in junction temperature with increasing particle volume fractions of Al_2O_3-water due to viscosity increase.

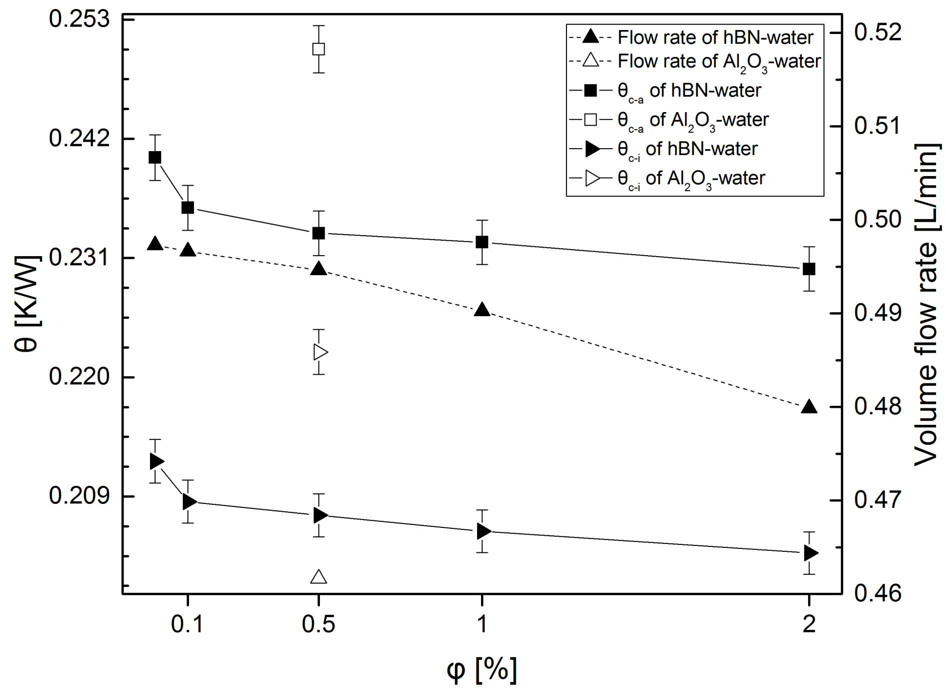

Figure 3.11. Effect of particle volume fraction of nanofluids on volume flow rate, case-to-ambient thermal resistance and cold plate thermal resistance

Figure 3.12 shows the change in normalized Stanton number for different hBN particle volume fractions, cold plates and flow rates with respect to normalized case-to-ambient thermal resistance. The data point on the far left of data set of each nanofluid concentration represents the data for 2 L/min flow rate and the flow rate decreases towards to right.

It can be clearly seen that nanofluid to base fluid case-to-ambient thermal resistance ratio and nanofluid to base fluid Stanton number ratio are correlated and correlation between these two parameters are represented by a linear fit as shown in 3.12. All data in the figure fall within the $\pm 5\%$ error band and the correlation can be used to predict cooling performance of hBN-water nanofluids for the systems con-

sidered. Therefore, it can be stated that the observed decrease in case-to-ambient resistance can be explained by increased heat transfer rate with respect to the increasing thermal capacity of the hBN nanofluid. Also the effect of hBN-water nanofluid concentration, cold plate type and volume flow rate on enhancement rates of Stanton number and thermal resistance of system are shown in Figure 3.13.

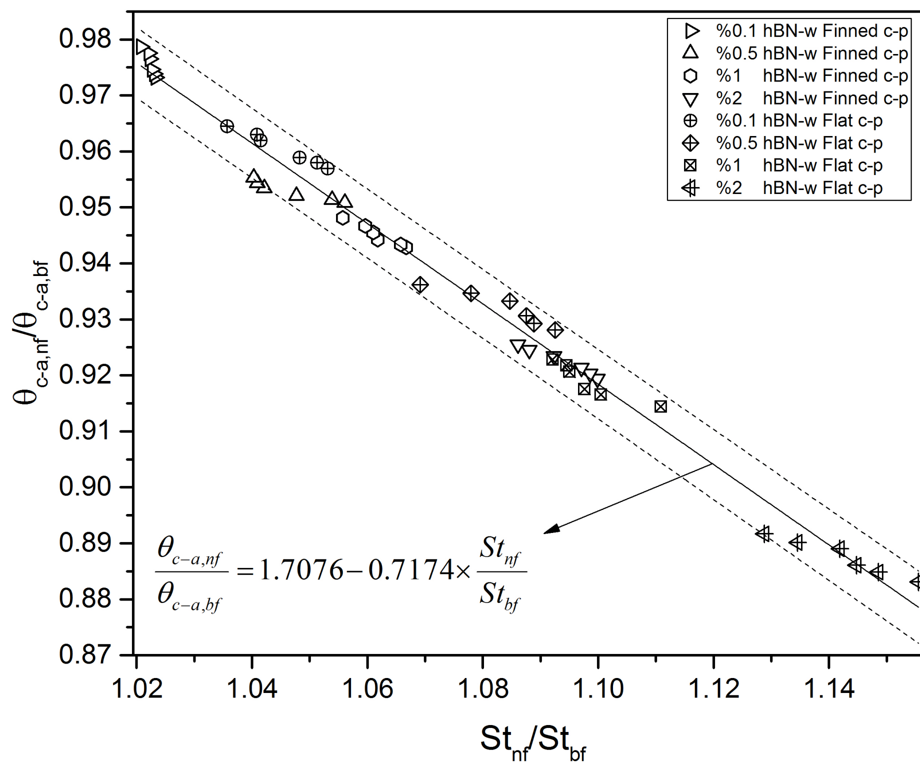

Figure 3.12. The change in normalized Stanton number for cold plate type, flow rate and hBN volume concentration

The thermal enhancement of hBN nanofluids for electronics cooling systems showed that the reduction in thermal resistance differ for each system due to different cold plate designs and nanofluid particle volume fractions. The effect of hBN nanofluid is relatively limited for the systems with higher heat transfer area due to denser fins, whereas the effect is more significant for the systems with limited heat transfer. Moreover, despite the decreasing flow rates due to increasing viscosity, using higher particle

fractions leads to a superior performance. An optimization study should be carried out to identify the optimal cold plate design and nanofluid. It is expected that the cooling performance could further improved by using an optimized cold plate and nanofluid.

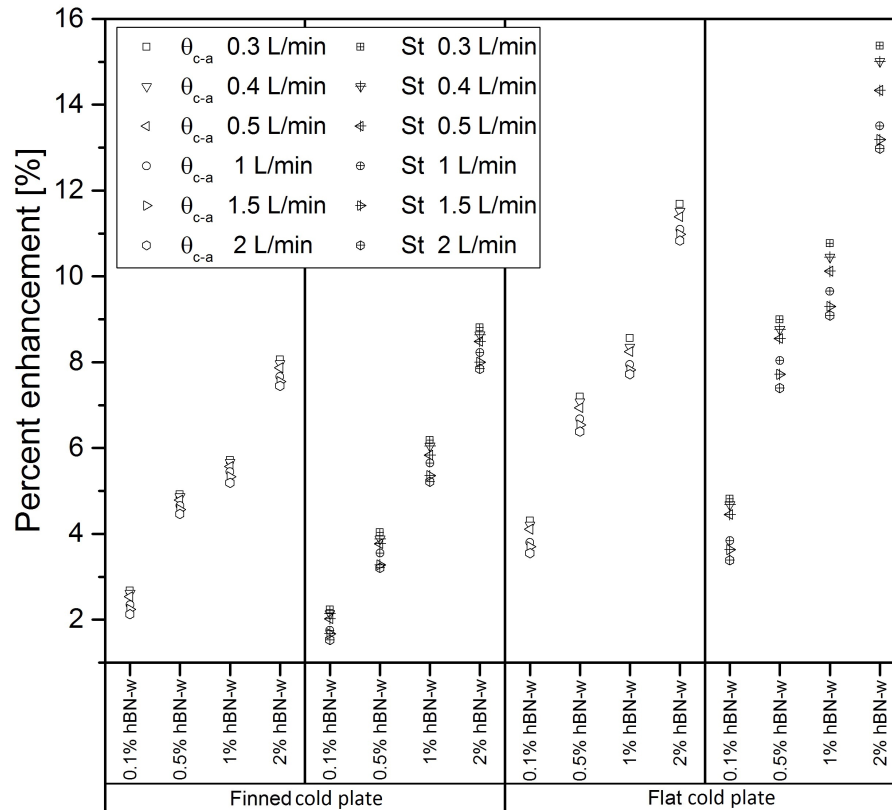

Figure 3.13. Enhancement rates of Stanton number and case-to-ambient thermal resistance for different volume concentrations of hBN-water nanofluids and volume flow rates

4. CONCLUSION AND FUTURE WORK

4.1. Conclusion

Heat transfer performance of hBN-water nanofluids is investigated with two different experimental cooling systems. While the first set of experiments rely on controlled flow rates between 0.3-2 L/min with two different cold plates, in the second set of experiments a commercial liquid cooling system with constant pumping power is used. The results are compared to that of DI-water and 0.5% Al_2O_3-water nanofluid to understand relative change in the heat transfer performance. The particle volume fractions considered are 0.1, 0.5, 1, 2% for hBN-water that are prepared by using two step method. Conductivity and viscosity of prepared nanofluids are measured before and after the experiments to ensure that experiments do not cause any deterioration in nanofluids' thermophysical properties.

Significant decrease in thermal resistances of system, cold plate and heat exchanger is observed when hBN-water nanofluids are used with respect to DI-water. Maximum enhancement in reduction of case-to-ambient thermal resistance is obtained by using hBN-water nanofluid with 2% volume fraction as 4.3% for commercial liquid cooling system, 7.8% and 11.2% for experimental cooling systems with finned and flat cold plates, respectively. Also maximum enhancement is found as 10% and 15.4% for finned and flat cold plate at 0.3 L/min flow rate for 2% hBN-water nanofluid, respectively. Results of different cold plates showed that Stanton number can be used to predict hBN-water nanofluids cooling performance.

Experimental results for Al_2O_3-water nanofluid with 0.5% volume fraction showed no improvement for controlled flow rate experiments and a deterioration in performance is observed for constant pumping power. The performance of Al_2O_3-water nanofluid in this study indicated that increase of thermal conductivity of nanofluid should be higher than its viscosity increase. The results of this study clearly showed that, hBN-water nanofluids can be used as working fluids in well-designed computer cooling applications

for such nanofluids to obtain maximum cooling performance.

4.2. Recommendations for Future Work

In this study, performance of nanofluids are investigated under constant flow rate and constant pumping power conditions for computer cooling systems. A further study can be carried out to obtain maximum cooling performance by using minimum resources. Meaning that, particle volume fraction of nanofluids can be reduced to use less pumping power by considering trade-off between viscosity increase and pumping power requirement.

Although enhancement rate increases with increasing particle volume fraction of hBN-water nanofluids, internal geometry of the cold plate has considerable effect on the overall liquid cooling performance as can be seen from the results of the experiments. A cold plate can be designed to get maximum efficiency in terms of heat transfer. Since cold plate thermal resistance comprises more than 80% of overall system' thermal resistance, required flow rate can be decreased to minimize pumping power requirement with a well designed cold plate.

Results of the experiments with commercial cooling system showed that viscosity increase has great affect on flow rate and thermal resistance at constant pumping power condition. Therefore another extension for this study could be pressure drop measurements to identify pressure drop characteristics of nanofluids which is mainly associated with particle volume fraction of nanofluids.

REFERENCES

1. Scott, A. W., *Cooling of electronic equipment*, Wiley-Interscience, 1974.

2. Hamilton, R. and O. Crosser, “Thermal conductivity of heterogeneous two-component systems”, *Industrial & Engineering chemistry fundamentals*, Vol. 1, No. 3, pp. 187–191, 1962.

3. Ahuja, A. S., “Augmentation of heat transport in laminar flow of polystyrene suspensions. I. Experiments and results”, *Journal of Applied Physics*, Vol. 46, No. 8, pp. 3408–3416, 1975.

4. Sohn, C. W. and M. Chen, “Microconvective thermal conductivity in disperse two-phase mixtures as observed in a low velocity Couette flow experiment”, *ASME J. Heat Transfer*, Vol. 103, pp. 47–51, 1981.

5. Das, S. K., S. U. Choi and H. E. Patel, “Heat transfer in nanofluids—a review”, *Heat Transfer Engineering*, Vol. 27, No. 10, pp. 3–19, 2006.

6. Choi, S., “Enhancing thermal conductivity of fluids with nanoparticles”, *ASME-Publications-Fed*, Vol. 231, pp. 99–106, 1995.

7. Karthikeyan, N., J. Philip and B. Raj, “Effect of clustering on the thermal conductivity of nanofluids”, *Materials Chemistry and Physics*, Vol. 109, No. 1, pp. 50–55, 2008.

8. Gupta, M., N. Arora, R. Kumar, S. Kumar and N. Dilbaghi, “A comprehensive review of experimental investigations of forced convective heat transfer characteristics for various nanofluids”, *International Journal of Mechanical and Materials Engineering*, Vol. 9, No. 1, pp. 1–21, 2014.

9. Tuckerman, D. B. and R. Pease, “High-performance heat sinking for VLSI”, *IEEE*

Electron device letters, Vol. 2, No. 5, pp. 126–129, 1981.

10. Fedorov, A. G. and R. Viskanta, "Three-dimensional conjugate heat transfer in the microchannel heat sink for electronic packaging", *International Journal of Heat and Mass Transfer*, Vol. 43, No. 3, pp. 399–415, 2000.

11. Li, J., G. Peterson and P. Cheng, "Three-dimensional analysis of heat transfer in a micro-heat sink with single phase flow", *International Journal of Heat and Mass Transfer*, Vol. 47, No. 19, pp. 4215–4231, 2004.

12. Chen, Y., C. Zhang, M. Shi and J. Wu, "Three-dimensional numerical simulation of heat and fluid flow in noncircular microchannel heat sinks", *International Communications in Heat and Mass Transfer*, Vol. 36, No. 9, pp. 917–920, 2009.

13. Dehghan, M., M. Daneshipour, M. S. Valipour, R. Rafee and S. Saedodin, "Enhancing heat transfer in microchannel heat sinks using converging flow passages", *Energy Conversion and Management*, Vol. 92, pp. 244–250, 2015.

14. Wang, H., Z. Chen and J. Gao, "Influence of geometric parameters on flow and heat transfer performance of micro-channel heat sinks", *Applied Thermal Engineering*, Vol. 107, pp. 870–879, 2016.

15. Nayak, D., L.-T. Hwang, I. Turlik and A. Reisman, "A high-performance thermal module for computer packaging", *Journal of Electronic Materials*, Vol. 16, No. 5, pp. 357–364, 1987.

16. Peng, X., G. Peterson and B. Wang, "Heat transfer characteristics of water flowing through microchannels", *Experimental Heat Transfer An International Journal*, Vol. 7, No. 4, pp. 265–283, 1994.

17. Zhang, H., D. Pinjala, T. Wong, K. Toh and Y. Joshi, "Single-phase liquid cooled microchannel heat sink for electronic packages", *Applied Thermal Engineering*, Vol. 25, No. 10, pp. 1472–1487, 2005.

18. Naphon, P. and S. Wiriyasart, "Liquid cooling in the mini-rectangular fin heat sink with and without thermoelectric for CPU", *International Communications in Heat and Mass Transfer*, Vol. 36, No. 2, pp. 166–171, 2009.

19. Wang, G., D. Niu, F. Xie, Y. Wang, X. Zhao and G. Ding, "Experimental and numerical investigation of a microchannel heat sink (MCHS) with micro-scale ribs and grooves for chip cooling", *Applied Thermal Engineering*, Vol. 85, pp. 61–70, 2015.

20. Timofeeva, E. V., A. N. Gavrilov, J. M. McCloskey, Y. V. Tolmachev, S. Sprunt, L. M. Lopatina and J. V. Selinger, "Thermal conductivity and particle agglomeration in alumina nanofluids: experiment and theory", *Physical Review E*, Vol. 76, No. 6, p. 061203, 2007.

21. Buongiorno, J., D. C. Venerus, N. Prabhat, T. McKrell, J. Townsend, R. Christianson, Y. V. Tolmachev, P. Keblinski, L.-w. Hu, J. L. Alvarado *et al.*, "A benchmark study on the thermal conductivity of nanofluids", *Journal of Applied Physics*, Vol. 106, No. 9, p. 094312, 2009.

22. Zhu, H., C. Zhang, S. Liu, Y. Tang and Y. Yin, "Effects of nanoparticle clustering and alignment on thermal conductivities of Fe 3 O 4 aqueous nanofluids", *Applied Physics Letters*, Vol. 89, No. 2, p. 023123, 2006.

23. Wang, J., R. Zheng, J. Gao and G. Chen, "Heat conduction mechanisms in nanofluids and suspensions", *Nano Today*, Vol. 7, No. 2, pp. 124–136, 2012.

24. Keblinski, P., S. Phillpot, S. Choi and J. Eastman, "Mechanisms of heat flow in suspensions of nano-sized particles (nanofluids)", *International Journal of Heat and Mass Transfer*, Vol. 45, No. 4, pp. 855–863, 2002.

25. Eapen, J., J. Li and S. Yip, "Mechanism of thermal transport in dilute nanocolloids", *Physical Review Letters*, Vol. 98, No. 2, p. 028302, 2007.

26. Jang, S. P. and S. U. Choi, "Role of Brownian motion in the enhanced thermal conductivity of nanofluids", *Applied Physics Letters*, Vol. 84, No. 21, pp. 4316–4318, 2004.

27. Prasher, R., P. E. Phelan and P. Bhattacharya, "Effect of aggregation kinetics on the thermal conductivity of nanoscale colloidal solutions (nanofluid)", *Nano Letters*, Vol. 6, No. 7, pp. 1529–1534, 2006.

28. Kumar, P. M., J. Kumar and S. Suresh, "Experimental investigation on convective heat transfer and friction factor in a helically coiled tube with Alˆ sub 2ˆ O3/water nanofluid", *Journal of Mechanical Science and Technology*, Vol. 27, No. 1, p. 239, 2013.

29. Akhavan-Zanjani, H., M. Saffar-Avval, M. Mansourkiaei, F. Sharif and M. Ahadi, "Experimental investigation of laminar forced convective heat transfer of Graphene–water nanofluid inside a circular tube", *International Journal of Thermal Sciences*, Vol. 100, pp. 316–323, 2016.

30. Pak, B. C. and Y. I. Cho, "Hydrodynamic and heat transfer study of dispersed fluids with submicron metallic oxide particles", *Experimental Heat Transfer an International Journal*, Vol. 11, No. 2, pp. 151–170, 1998.

31. Piratheepan, M. and T. Anderson, "An experimental investigation of turbulent forced convection heat transfer by a multi-walled carbon-nanotube nanofluid", *International Communications in Heat and Mass Transfer*, Vol. 57, pp. 286–290, 2014.

32. Sommers, A. D. and K. L. Yerkes, "Experimental investigation into the convective heat transfer and system-level effects of Al2O3-propanol nanofluid", *Journal of Nanoparticle Research*, Vol. 12, No. 3, pp. 1003–1014, 2010.

33. Ding, Y., H. Chen, Y. He, A. Lapkin, M. Yeganeh, L. Šiller and Y. V. Butenko, "Forced convective heat transfer of nanofluids", *Advanced Powder Technology*,

Vol. 18, No. 6, pp. 813–824, 2007.

34. Duangthongsuk, W. and S. Wongwises, "An experimental study on the heat transfer performance and pressure drop of TiO 2-water nanofluids flowing under a turbulent flow regime", *International Journal of Heat and Mass Transfer*, Vol. 53, No. 1, pp. 334–344, 2010.

35. Koo, J. and C. Kleinstreuer, "Laminar nanofluid flow in microheat-sinks", *International Journal of Heat and Mass Transfer*, Vol. 48, No. 13, pp. 2652–2661, 2005.

36. Jang, S. P. and S. U. Choi, "Cooling performance of a microchannel heat sink with nanofluids", *Applied Thermal Engineering*, Vol. 26, No. 17, pp. 2457–2463, 2006.

37. Mital, M., "Semi-analytical investigation of electronics cooling using developing nanofluid flow in rectangular microchannels", *Applied Thermal Engineering*, Vol. 52, No. 2, pp. 321–327, 2013.

38. Khaleduzzaman, S., R. Saidur, I. Mahbubul, T. Ward, M. Sohel, I. Shahrul, J. Selvaraj and M. Rahman, "Energy, Exergy, and Friction Factor Analysis of Nanofluid as a Coolant for Electronics", *Industrial & Engineering Chemistry Research*, Vol. 53, No. 25, pp. 10512–10518, 2014.

39. Vanaki, S. M., P. Ganesan and H. Mohammed, "Numerical study of convective heat transfer of nanofluids: A review", *Renewable and Sustainable Energy Reviews*, Vol. 54, pp. 1212–1239, 2016.

40. Chein, R. and J. Chuang, "Experimental microchannel heat sink performance studies using nanofluids", *International Journal of Thermal Sciences*, Vol. 46, No. 1, pp. 57–66, 2007.

41. Ho, C.-J., L. Wei and Z. Li, "An experimental investigation of forced convective cooling performance of a microchannel heat sink with Al 2 O 3/water nanofluid", *Applied Thermal Engineering*, Vol. 30, No. 2, pp. 96–103, 2010.

42. Escher, W., T. Brunschwiler, N. Shalkevich, A. Shalkevich, T. Burgi, B. Michel and D. Poulikakos, "On the cooling of electronics with nanofluids", *Journal of heat transfer*, Vol. 133, No. 5, p. 051401, 2011.

43. Yu, L. and D. Liu, "Study of the Thermal Effectiveness of Laminar Forced Convection of Nanofluids for Liquid Cooling Applications", *IEEE Transactions on Components, Packaging and Manufacturing Technology*, Vol. 3, No. 10, pp. 1693–1704, 2013.

44. Sohel, M., S. Khaleduzzaman, R. Saidur, A. Hepbasli, M. Sabri and I. Mahbubul, "An experimental investigation of heat transfer enhancement of a minichannel heat sink using Al 2 O 3–H 2 O nanofluid", *International Journal of Heat and Mass Transfer*, Vol. 74, pp. 164–172, 2014.

45. Lai, W., B. Duculescu, P. Phelan and P. Prasher, "A review of convective heat transfer with nanofluids for electronics packaging", *Thermal and Thermomechanical Phenomena in Electronics Systems, 2006. ITHERM'06. The Tenth Intersociety Conference on*, pp. 5–pp, IEEE, 2006.

46. Nguyen, C. T., G. Roy, C. Gauthier and N. Galanis, "Heat transfer enhancement using Al 2 O 3–water nanofluid for an electronic liquid cooling system", *Applied Thermal Engineering*, Vol. 27, No. 8, pp. 1501–1506, 2007.

47. Townsend, J. and R. J. Christianson, "Nanofluid properties and their effects on convective heat transfer in an electronics cooling application", *Journal of Thermal Science and Engineering Applications*, Vol. 1, No. 3, p. 031006, 2009.

48. Roberts, N. A. and D. Walker, "Convective performance of nanofluids in commercial electronics cooling systems", *Applied Thermal Engineering*, Vol. 30, No. 16, pp. 2499–2504, 2010.

49. Putra, N., F. N. Iskandar *et al.*, "Application of nanofluids to a heat pipe liquid-block and the thermoelectric cooling of electronic equipment", *Experimental Ther-*

mal and Fluid Science, Vol. 35, No. 7, pp. 1274–1281, 2011.

50. Rafati, M., A. Hamidi and M. S. Niaser, "Application of nanofluids in computer cooling systems (heat transfer performance of nanofluids)", *Applied Thermal Engineering*, Vol. 45, pp. 9–14, 2012.

51. Selvakumar, P. and S. Suresh, "Convective performance of CuO/water nanofluid in an electronic heat sink", *Experimental Thermal and Fluid Science*, Vol. 40, pp. 57–63, 2012.

52. Nazari, M., M. Karami and M. Ashouri, "Comparing the thermal performance of water, Ethylene Glycol, Alumina and CNT nanofluids in CPU cooling: Experimental study", *Experimental Thermal and Fluid Science*, Vol. 57, pp. 371–377, 2014.

53. Li, Y., J. Zhou, Z. Luo, S. Tung, E. Schneider, J. Wu and L. Xiaojing, "Investigation on two abnormal phenomena about thermal conductivity enhancement of BN/EG nanofluids", *Nanoscale Res. Lett.*, Vol. 6, p. 443., 2011.

54. Guo, J., Z. Guo, X. Wang, Y. Li and Q. Lv, "Experimental Investigation on Thermophysical Performance of BN/EG Nanofluids Influenced by Dispersant.", *Applied Mechanics & Materials*, Vol. 757, 2015.

55. İlhan, B., M. Kurt and H. Ertürk, "Experimental investigation of heat transfer enhancement and viscosity change of hBN nanofluids", *Experimental Thermal and Fluid Science*, Vol. 77, pp. 272–283, 2016.

56. İlhan, B. and H. Ertürk, "Experimental characterization of laminar forced convection of hBN-water nanofluid in circular pipe", *International Journal of Heat and Mass Transfer*, Vol. 111, pp. 500–507, 2017.

57. Kline, S. J. and F. McClintock, "Describing uncertainties in single-sample experiments", *Mechanical Engineering*, Vol. 75, No. 1, pp. 3–8, 1953.

58. Yoo, D.-H., K. Hong and H.-S. Yang, "Study of thermal conductivity of nanofluids for the application of heat transfer fluids", *Thermochimica Acta*, Vol. 455, No. 1, pp. 66–69, 2007.

APPENDIX A: TECHNICAL DRAWINGS

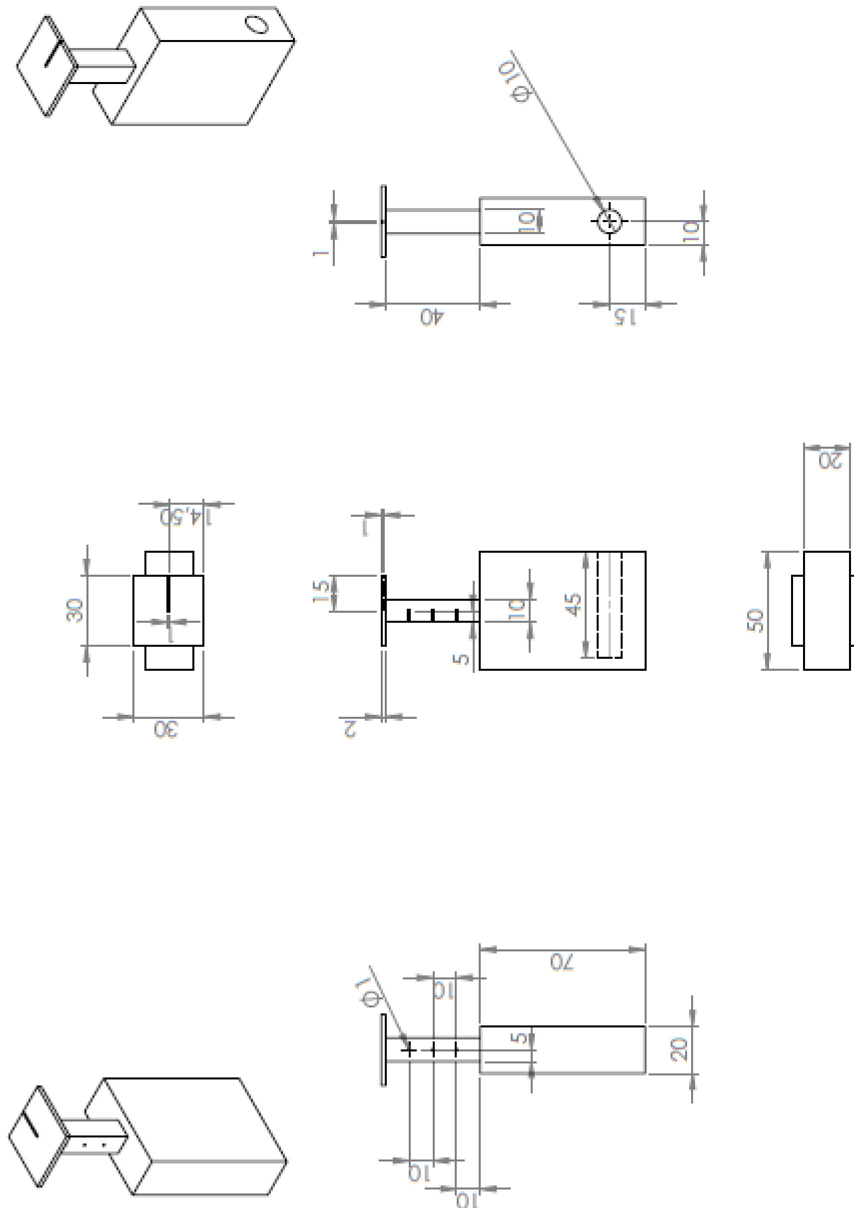

Figure A.1. Technical drawing of copper heater block